[redacted]

RES/FSCB 2019-01

Independent MELCOR Confirmatory Analysis for NuScale Small Modular Reactor

S. Campbell
H. Esmaili
J. Schaperow[1]

April 2019

Fuel and Source Term Code Development Branch
Division of Systems Analysis
Office of Nuclear Regulatory Research
United States Nuclear Regulatory Commission

[1] PRA and Severe Accidents Branch, Division of Safety Systems and Risk Assessment, Office of New Reactors, U.S. NRC

[redacted]

[redacted]

ACKNOWLEDGEMENTS

The authors would like to acknowledge A. Hathaway (NRC/RES) and Z. Yuan, S. Choi, A. Krall, and M. Khatib-Rahbar (Energy Research, Inc.) for their effort to develop the MELCOR model of NuScale.

[redacted]

[redacted]

TABLE OF CONTENTS

[redacted]

[redacted]

List of Tables

[redacted]

[redacted]

List of Figures

[redacted]

[redacted]

[redacted]

[redacted]

List of Acronyms

BAF	Bottom of Active Fuel
CDF	Core Damage Frequency
CE	Combustion Engineering
CNV	Containment Vessel
CVCS	Chemical and Volume Control System
DCA	Design Certification Application
DF	Decontamination Factor
DHRS	Decay Heat Removal System
EAB	Exclusion Area Boundary
ECCS	Emergency Core Cooling System
FSAR	Final Safety Analysis Report
IAB	Inadvertent Actuation Block
iPWR	integral Pressurized Water Reactor
LOCA	Loss of Coolant Accident
LPZ	Low Population Zone
MSIV	Main Steam Isolation Valve
NRC	Nuclear Regulatory Commission
PRA	Probabilistic Risk Assessment
PWR	Pressurized Water Reactor
PZR	Pressurizer
RCS	Reactor Coolant System
RPV	Reactor Pressure Vessel
RRV	Reactor Recirculation Valve
RSV	Reactor Safety Valve
RVV	Reactor Vent Valve
SA	Severe Accident
SG	Steam Generator
SGTR	Steam Generator Tube Rupture
SMR	Small Modular Reactor
TAF	Top of Active Fuel

[redacted]

[redacted]

Intentionally left blank

[redacted]

[redacted]

1. Introduction

This report documents the NRC staff's independent, confirmatory analysis of the severe accident simulations performed by NuScale Power, LLC. While the date of this report is April 2019, it was largely completed in the summer of 2018. The applicant's data cited and referenced in this report do not reflect updates or changes since that time.

1.1. NuScale small modular reactor

NuScale Power LLC submitted their Standard Design Certification Application (DCA) to the NRC for the NuScale Small Modular Reactor design in December 2016 (Reference 1). The NuScale Small Modular Reactor (SMR) is an integral Pressurized Water Reactor (iPWR) with a rated thermal power of 160 MW(t) and an electrical power output of 50 MW(e). The reactor coolant system (RCS) consists of a single, integrated reactor pressure vessel (RPV) that contains the reactor core, steam generators, and pressurizer. The steam generators (SG) consist of helical coils where, unlike large operating PWRs, primary side coolant flows on the outside of the tubes with steam being generated within the tubes. The containment consists of a steel vessel (referred to as the CNV) that is held at a vacuum during normal operations. There are no reactor coolant pumps used for forced flow through the core as the design depends upon buoyancy driven natural circulatory flow.

The NuScale SMR design includes an ECCS which provides protection for loss of coolant accidents. It consists of two Reactor Recirculation Valves (RRVs) toward the bottom of the RPV and three Reactor Vent Valves (RVVs) at the top of the RPV. Each valve includes an Inadvertent Actuation Block (IAB) which prevents the valve from opening until the differential pressure between the RPV and CNV is sufficiently low. Upon ECCS actuation, all five of these valves receive a signal to open. Once the IAB clears, the valves open and form a natural convection loop where steam escaping the RVVs condenses on the cooler CNV inner wall and re-enters the RPV through the RRVs. The Decay Heat Removal System (DHRS) is a heat exchanger that, when activated, passively removes decay heat via the steam generators into the reactor pool outside of containment.

1.2. Guidance for staff confirmatory analysis

Section 19.0, "Probabilistic Risk Assessment and Severe Accident Evaluation for New Reactors," of NUREG-0800, "Standard Review Plan" states the following:

> "For DC applications and COL applications not referencing the Level 2 PRA in the DC, the reviewer[6] carries out an independent assessment of the plant response to selected severe accident scenarios using the latest version of the MELCOR computer code. The assessment should examine accident scenarios from the PRA, which are chosen based on a combination of frequency, consequence, and dominant risk. Some of these scenarios should be similar or identical to sequences analyzed by the applicant and reported in the PRA. The reviewer compares the results of corresponding sequences and release categories in the two studies. If the results of the assessment do not support and confirm the applicant's simulation of the accident progression, analysis methodology, and interpretations of its analyses of the reactor, containment, and system

[redacted]

[redacted]

response to severe accidents, the reviewer engages with the applicant to resolve the differences in results.

[6] Support from an independent contractor or staff in the Office of Research may be necessary."

The staff followed the above Standard Review Plan 19.0 guidance in performing its independent confirmatory analysis. In addition, the staff used results from one of the scenarios to assist the staff in evaluating the NuScale Accident Source Term Methodology Topical Report (Reference 5).

1.3. Outline of this report

Section 2 provides an overview of the NuScale design, the modeling approach used in the MELCOR input deck and a description of the process used for selecting the scenarios used for the staff's independent confirmatory analysis. Section 3 presents the staff's MELCOR results for each of the selected scenarios and includes comparisons to NuScale's MELCOR results. Section 4 gives the results of sensitivity calculations that were conducted by the staff. Finally, Section 5 provides results from one of the scenarios to assist the staff in evaluating the NuScale Accident Source Term Methodology Topical Report.

[redacted]

[redacted]

Intentionally left blank

[redacted]

[redacted]

2. MELCOR Modeling Approach and Scenario Selection

2.1. Staff's MELCOR Modeling Approach

Table 2.1 lists design features of the NuScale SMR and compares them with those of a representative Combustion Engineering operating reactor (Calvert Cliffs, Reference 2).

Table 2.1 Comparison of select design features of the NuScale to a representative Combustion Engineering operating reactor

Parameter	NuScale (Reference 1)	Calvert Cliffs (Reference 2)
Core rated thermal power (MWt)	160	2,560
Number of external loops	0	2
Number of Reactor Coolant Pumps	0	4
Steam Generator Type	Helical Coil	U-tube
Number of SG tubes (per SG)	1,380	8,471
Core active length (m)	2.0	3.47
Primary operating pressure (psia)	1,850	2,250
Core flow rate (kg/s)	587	15,400
Total Coolant Volume (m^3)	75	314
Core inlet temperature (C)	258	285
Core outlet temperature (C)	310	315
Number of Fuel Assemblies	37	217
Number of Control Assemblies	16	77
Mass of fuel (kg)	9,232	94,016
Containment Type	Steel cylindrical vessel	Reinforced concrete with steel liner
Containment free volume (m^3)	180	56,634
Containment design pressure (psig)	1,000	50

The staff performed its calculations using MELCOR version 2.2 sub-version 10284. The MELCOR model was developed by the staff's contractor Energy Research Inc. to be a realistic representation of the design and its operation by using plant design data given in the NuScale FSAR and other sources. The MELCOR model is documented in Reference 3. The model consists of 78 control volumes for the reactor vessel, steam generators, containment vessel, and reactor pool, and the associated safety systems. It also consists of 130 flow paths connecting these volumes. Figure 2.1 through Figure 2.4 give the detailed nodalization for the pressure vessel, the reactor coolant system, containment, and the core respectively.

Figure 2.1 shows the nodalization of the reactor pressure vessel. Also included in this figure are the two steam generators (SG) with volumes 301-304 representing SG1 and 351-354 representing SG2.

Figure 2.2 shows the containment vessel nodalization and Figure 2.3 shows the nodalization of the reactor pool. Not shown is CV599 which models the rest of the reactor pool containing the other 11 reactor modules and is fully connected to the outer volumes in Figure 2.3. The large

[redacted]

[redacted]

volume of CV599 does consider the other modules that may exist in the reactor building but simply acts as a large heat sink for the single module that is modeled.

As shown in Figure 2.4, the core and lower plenum regions are divided into four radial rings in the MELCOR COR package. In the core region, three of the rings represent the active fuel. The core and lower plenum regions are also divided into 12 axial nodes. The active fuel makes up 6 of these axial nodes, the lower support area makes up 2, and the lower plenum makes up 3.

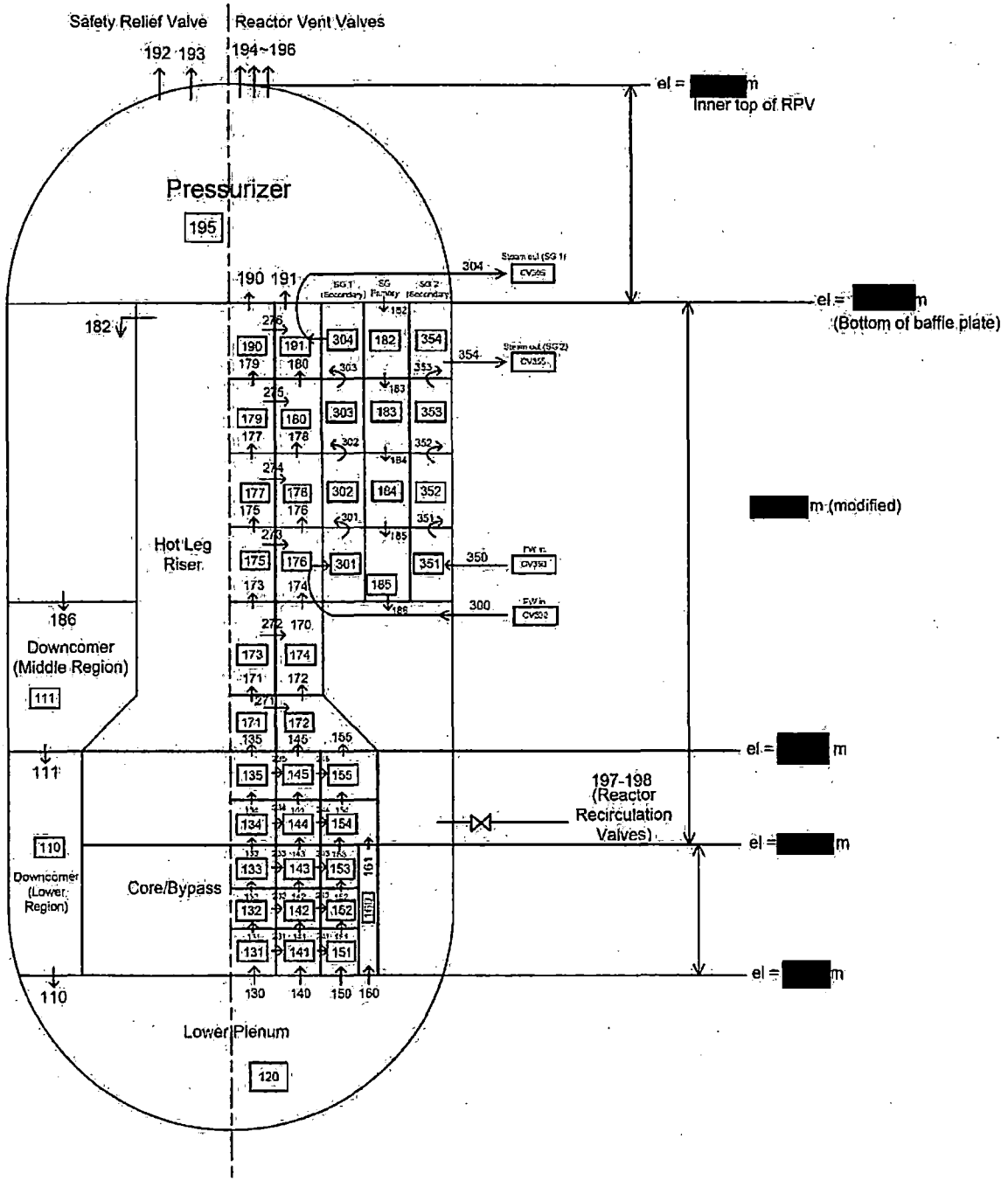

Figure 2.1 Staff's MELCOR nodalization for NuScale model – Reactor Vessel

[redacted]

[redacted]

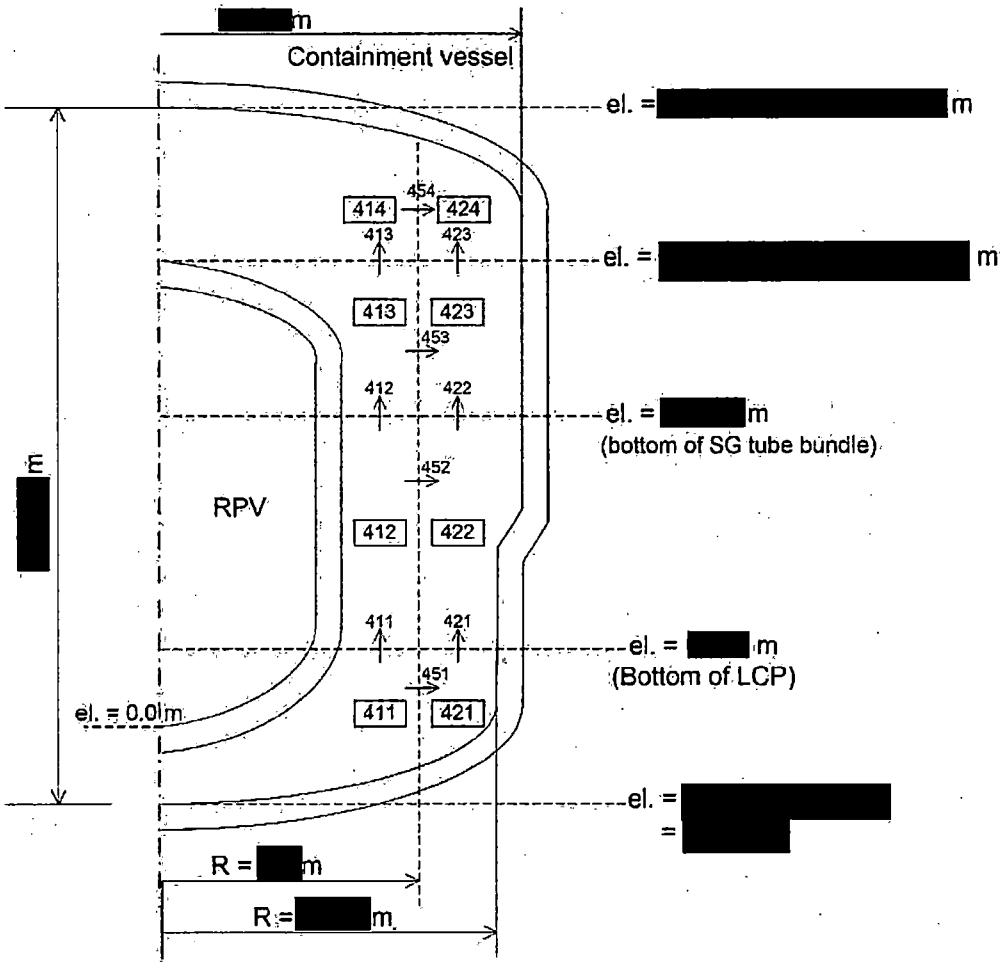

Figure 2.2 Staff's MELCOR nodalization for NuScale model – Containment Vessel

[redacted]

[redacted]

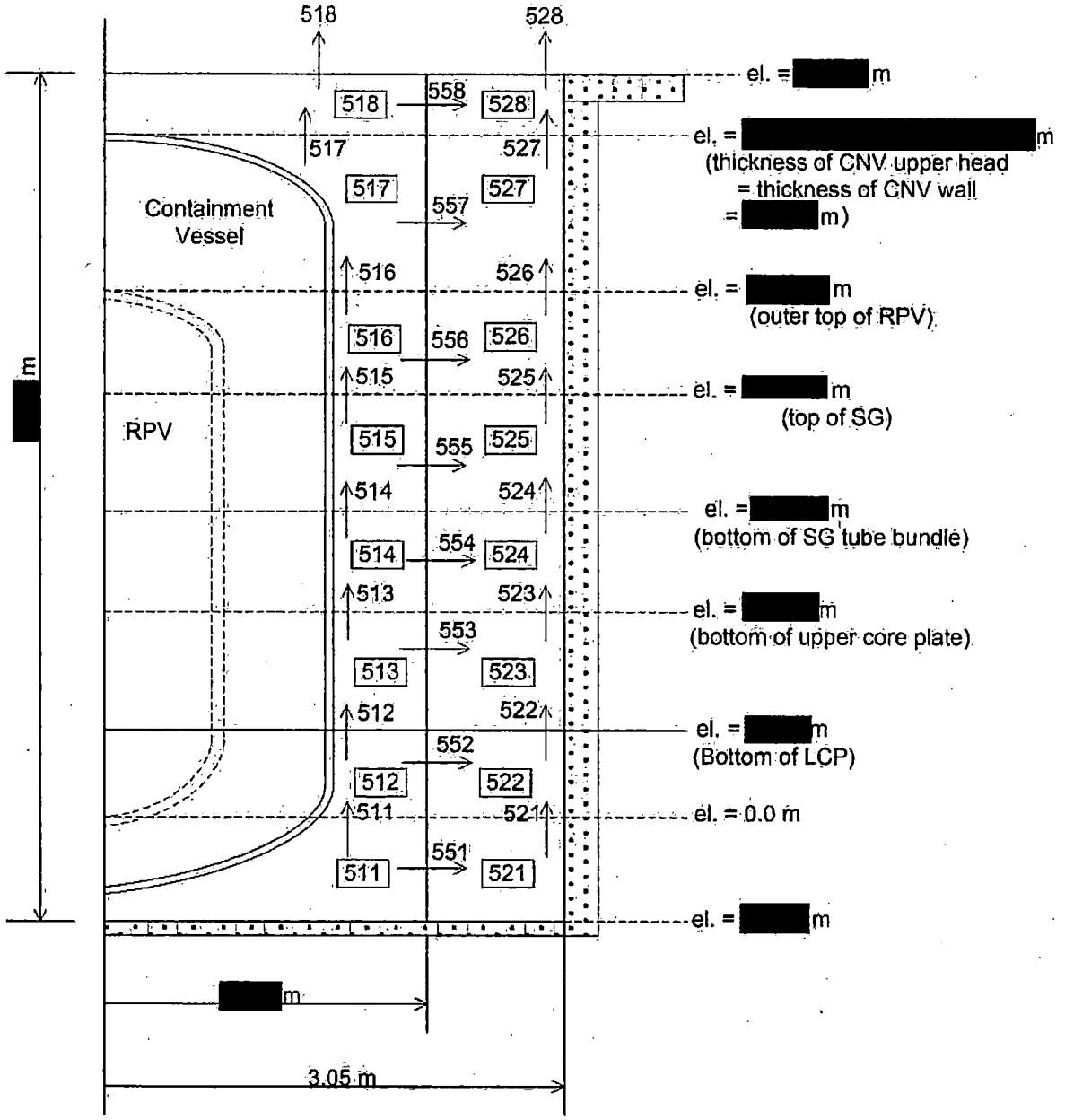

Figure 2.3 Staff's MELCOR nodalization for NuScale model – Reactor bay water pool

[redacted]

[redacted]

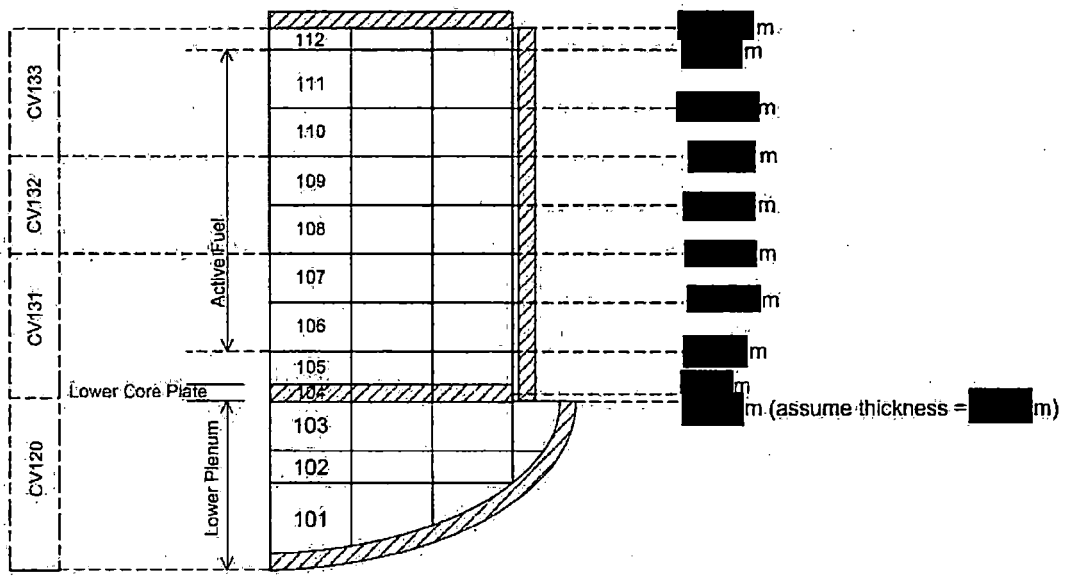

Figure 2.4 Staff's MELCOR nodalization for NuScale model – COR package

2.2. Selection of Accident Scenarios

Per Standard Review Plan 19.0 guidance, the staff reviewed the applicant's documentation to identify the sequences analyzed by the applicant and reported in the PRA. The staff reviewed FSAR Chapter 19 (Reference 1), the Environmental Report (Reference 4), the NuScale Accident Source Term Methodology Topical Report (Reference 5) and underlying supporting documents made available to the staff in the applicant's electronic reading room as part of two regulatory PRA audits. Table 2.2 lists the base-case scenarios analyzed by the applicant. The first section of the table that is shaded in gray lists the MELCOR analyses performed for FSAR Chapter 19 for PRA and severe accident analysis. In FSAR Chapter 19, the applicant chose scenarios to understand the range of plant responses to beyond-design-basis accidents. The applicant analyzed scenarios with a hole in the top of the RCS (a vapor space break), a hole in the side of the RCS (a liquid space break), and a CVCS line break outside of containment (a containment bypass scenario). The applicant used the results of these simulations as input to analyses of in-vessel retention, steam explosion, high pressure melt ejection, and thermally induced steam generator tube failure. The applicant performed additional MELCOR and MACCS calculations assuming the module is lying on its side at the bottom of the reactor pool to show that module drop accidents do not result in a large release. (The module drop accident is not shaded in gray and was analyzed in Chapter 19 and in the Environmental Report.) The detailed rationale for scenario selection is given in Reference 6.

[redacted]

Table 2.2 Compilation of MELCOR calculations performed by NuScale

Analysis	Underlying supporting document	Case number	MEL-COR	Hole(s) in RCS				Injection and cooling			Sensitivity Cases	CDF[1] (/yr)
				Break location	By-pass	ECCS valves open	RSV	CVCS	CFDS	DHRS		
PRA and SA analysis (FSAR Chapter 19)	ER-P060-4715	TRN 07T	2.1				SO					1.5E-11
	ER-P060-4748	LEC 06T				3 RVVs	✓				DHRS	
	ER-P060-4749	LCC 05T		CVCS in cont.[a]		3 RVVs	✓				DHRS	7.0E-12
	ER-P060-4857	LCC 05T		CVCS in cont.[a]			✓				Reduced area	
	ER-P060-4750	LCU 03T		CVCS outside cont.[b]	✓		✓				CFDS	1.7E-11
SAMDA (Environ-mental Report)	ER-P060-7085	Module drop	1.8.6[c]			All					Hole size	5.3E-7
	ER-P030-4527	LEC 05T (RC4)				3 RVVs	✓					2.4E-9
	ER-P030-4529	TRN 07T (RC6)				3 RVVs	SO					2.1E-10
	ER-P030-4530	TRN 08T (RC7)		PZR heater access port [redacted] in^2)		3 RVVs						2.7E-10
	ER-P030-4525	LCC 05T (RC1)		CVCS in cont.[b]		3 RVVs	✓					2.2E-11
	ER-P030-4526	LCU 03T (RC3)		CVCS outside cont.[b]	✓							1.7E-11
	ER-P030-4524	LCI 05T (RC2)		CVCS outside cont.[b]	✓	3 RVVs						1.1E-12
	ER-P030-4528	LSU 06T (RC5)		SGTF & secondary line	✓		✓					1.4E-13
Siting (Accident Source Term Methodology TR)	EE-P060-3637 (superseded)	4	1.8.6[c]			2 RVVs				✓		
		3				2 RRVs						
		2		CVCS in cont.[b]		2 RVVs						
		1		CVCS in cont.[b]		2 RRVs				✓		
	EE-P060-5275	5	2.1			3 RVVs				✓		
		4				2 RRVs				✓		
		1		CVCS in cont.[a]						✓		
		3		CVCS in cont.[a]		3 RVVs				✓		
		2		CVCS in cont.[a]		2 RRVs				✓		

1 The CDF values shown for the PRA and SA analysis (FSAR Chapter 19) are for internal events. The CDF values shown for SAMDA (Environmental Report) are for the range of hazards and represent the sum of the sequences associated with the release category.

a Charging line break at [redacted] ft elevation with [redacted] in^2 hole area.
b Charging line break at [redacted] ft elevation with [redacted] in^2 hole area.
c This is an earlier version of the code that no longer under active development

CVCS line breaks are assumed to be on the injection side.
ER-P060-7085 is used for both the Chapter 19 and SAMDA analysis.
CDF values are taken from the following sources:
- the SAMDA values are from Table B-17 of the Environmental Report
- the ER-P060-4715 value is from Table 19.1-17 of the FSAR
- the ER-P060-4749/ER-P060-4857 and ER-P060-4750 values are from Figure 19.1-13 of the FSAR
EE-P060-3637 is based on an older version of the NuScale design. Differences include number and size of ECCS valves and IAB setpoint.
EE-P060-5275 assumes DHRS deactivates when core damage starts.

The staff reviewed the scenarios and their CDFs listed in Table 2.2 to select scenarios for confirmatory analysis. The available CDFs for Chapter 19 were the internal events CDF. The available CDFs for the Environmental Report were integrated CDFs for the range of initiators analyzed by the applicant. The Source Term Topical Report did not provide CDFs. Because of the availability of integrated CDFs from the Environmental Report and the overlap between the scenarios analyzed for the Environmental Report and the other two areas (Chapter 19 and Siting), the staff used the CDFs from the Environmental Report to select scenarios as discussed below.

The highest CDF scenario is the module drop accident. The module-drop analysis for both the Environmental Report and Chapter 19 is documented in Reference 7. Because of the importance of reactor pool scrubbing in determining the environmental release for this scenario, the staff did not see a need to perform MELCOR confirmatory calculations with the module on its side. The staff instead chose to focus its review on the applicant's evaluation of reactor pool scrubbing. The staff's review of the applicant's evaluation of reactor pool scrubbing is document in the staff's SER.

The next highest CDF scenario is a spurious RVV opening with partial ECCS actuation (remaining 2 RVVs open and no RRVs open) with DHRS unavailable. This scenario was also analyzed for Chapter 19 (LEC-06T in Table 2.2). A similar scenario was analyzed for Siting, but the Siting scenario included DHRS. The staff selected this scenario (without DHRS) for MELCOR confirmatory analysis.

The two next highest CDF scenarios are a) 3 RVVs open plus pressurizer heater port failure and b) 3 RVVs open plus stuck-open reactor safety valve. These two scenarios are similar to the 3 RVVs open scenario already being assessed in the staff's confirmatory analysis (see paragraph above), because these two scenarios have similar hole sizes and hole elevations to the 3 RVVs open scenario. Therefore, the staff did not select these two scenarios for confirmatory analysis.

The next highest CDF scenario is a CVCS line break inside containment with 3 RVVs open (RRVs fail to open). This scenario also was analyzed for Chapter 19 (LCC-05T in Table 2.2) and Siting. The staff selected this scenario for MELCOR confirmatory analysis because of the uniqueness of the CVCS break which is low in the RPV (i.e., a liquid break).

The next highest CDF scenario is the CVCS line break outside containment. This scenario also was analyzed in Chapter 19 (LCU-03T in Table 2.2) and has the largest source term. The staff selected this scenario for confirmatory analysis.

NuScale also analyzed a steam generator tube failure accident resulting in containment bypass. However, this scenario was not chosen for confirmatory analysis, because its CDF is lower than the CVCS line break outside containment.

A summary of the scenarios selected for confirmatory analysis is given in Table 2.3

The staff applied its MELCOR model to each of the scenarios in Table 2.3. The staff compared the results of each its MELCOR simulations with the results for applicant's MELCOR simulations. The detailed results provided by the applicant in References 9 and 10 were used for the comparison. The results of the comparisons are given in the Section 3.

[redacted]

Table 2.3 Scenarios Selected for Confirmatory Analysis

Scenario	Environmental Report	Chapter 19	Chapter 15	CDF (per year)[1]
3 RVVs open[2]	✓	✓	✓	2.4E-9
CVCS break plus 3 RVVs open[2]	✓	✓	✓	2.2E-11
CVCS break outside containment[2]	✓	✓		1.7E-11

[1]The CDF values shown are for SAMDA (Environmental Report) and are for the range of hazards and represent the sum of the sequences associated with the release category.
[2]The staff's confirmatory analysis assumes DHRS does not operate.

[redacted]

[redacted]

3. MELCOR Results and Comparison with the Applicant's Results

This section presents the staff's independent MELCOR analysis with comparisons to the applicant's results. Additional staff sensitivity MELCOR analysis are given in Section 4 of this report.

3.1. LEC-06T

This scenario, referred to as LEC-06T in the applicant's FSAR, is initiated by the spurious opening of a single RVV followed by partial actuation of the ECCS (other two RVVs open but both RRVs remain closed). The DHRS is assumed to be unavailable.

A summary of the key event timings is given in Table 3.1. Figure 3.1 through Figure 3.11 compare the simulation results of the staff and applicant. In the following discussion, the numbers cited are for the staff's MELCOR simulations unless otherwise stated.

Figure 3.1 shows the pressure in the RPV, CNV and SG in the first 15 minutes of the accident. When the first RVV opens spuriously at time 0, the RPV and CNV pressures equalize after 2 minutes. Even though all three of the RVVs are open by 0.6 hours, it takes 1.6 hours and 2.6 hours for the RPV pressure to decrease to 200 psi and 100 psi, respectively. After 2 minutes, flow from the RCS to containment is primarily steam that is generated in the core, enters containment and is condensed on the containment inner surface. Containment (along with RCS) pressure drops below atmospheric pressure at 7.9 hours due to this condensation. As for the SGs, pressure initially spikes upon closure of the MSIVs and then drops with the corresponding drop in temperature in the SG.

Figure 3.2 shows the long-term pressure in the RPV, SGs (the two SGs are identical and therefore conditions within are identical as well), and CNV. Since the SG MSIVs close when the reactor trips, the SGs become isolated. When core damage and relocation occur, the temperature of the SGs slowly increases. Consequently, the pressure in the SGs also increases, rising to the SG relief valve setpoint around 23 hours, passing additional water to containment. As for the RPV, it is open to containment via the 3 open RVVs so its pressure is the same as the CNV and lower than that of the SGs.

When the RPV water level falls below the bottom of the SGs at 1.4 hours, the rate of cooling decreases since the SGs are hydraulically isolated. Consequently, the rate of depressurization in the SGs also slows. This phenomena is not as apparent in the applicant's calculations where the SG temperature and pressure continue to decrease at a similar rate after the water level falls below the SGs. The difference in SG pressure between the staff and applicant's calculations was discussed during an audit beginning March 6, 2018 (Reference 11). The applicant confirmed that no valves or systems (such as DHRS) had been left open. The applicant suggested it could be related to the staff's model not including heat transfer from the pipes connected to the SG (i.e., feed lines and steam lines) to the containment atmosphere whereas the applicant did include these structures.

The applicant's RPV and CNV pressure is lower than what is predicted by the staff (about 30% lower) in the first few minutes. Several explanations for this difference were posited and led to sensitivity calculations which are documented in Section 4. One explanation for the difference in pressure is that the RVV flow areas and form loss coefficients are different between the staff

[redacted]

and applicant's MELCOR input models. The staff requested as part of the 2017 PRA and severe accident audit (Reference 12) from the applicant the flow area of the RVVs and found that it had changed since the applicant had performed their MELCOR calculations. Staff used the new flow area in the confirmatory calculations and, as a result, the RVV flow area used in the staff's deck is smaller than that in the applicant's deck (17.3 in^2 versus [redacted] in^2). The sensitivity calculations documented in Section 4 showed that this difference in valve size had little impact on the early pressure difference and the integrated flow of water mass lost through the ECCS valves did not differ greatly from the base case, even in the long-term. Another sensitivity study documented in Section 4 brought to light another possible reason the early differences in RPV, CNV, and SG pressure. By increasing the number of nodes of the SGs both on the primary and secondary side, there was an increase in heat transfer from primary to secondary and the SG pressure slightly faster in the first few minutes of the transient, as shown in sensitivity calculations documented in Section 4. However, this too does not fully account for the differences in pressure.

Shown in Figure 3.3, there is a small difference in total core power between the staff and the applicant. Figure 3.4 gives the predicted water levels with an associated image of the NuScale vessel for perspective. The RPV water level decreases rapidly with the first RVV opening since liquid water is passed initially (see Figure 3.5). From then on, the water level decreases steadily with steam passing through the three open RVVs to the containment where it condenses and partially fills the CNV. RPV water level reaches the top of active fuel (TAF) at 5.3 hours (this is the collapsed level, the swollen level reaches TAF at 6.7 hours). Figure 3.6 gives the overall mass balance of water (steam and liquid water) in the RPV, CNV, and SGs and demonstrates the exchange of water between the three components. The drop in water mass in the SGs around 24 hours in the staff's calculations corresponds to the steam generator relief valve opening on high secondary pressure and relieving into containment.

Following core uncovery, core heat up and degradation occurs (see Figure 3.7 and Figure 3.8). Cladding oxidation begins at 8.7 hours (Figure 3.9) and gap release in ring one of the core occurs at 8.8 hours. In the staff's deck, the core is nodalized as three radial rings with 9, 14, and 14 assemblies respectively. In the applicant's deck, the core is nodalized as four radial rings with [redacted], and [redacted] assemblies respectively. In the staff's calculation, the two upper levels of ring 1collapse at 10 hours followed closely by the top level of ring 2 collapsing. It remains in this state until around 18 hours when the remainder of the first ring collapses due to loss of strength as a result of being at a high temperature for an extended period of time. The remainder of ring 2 then heats to the point of collapse as well.

In the staff's calculations, up until the time of core damage, water in the RPV core region, lower plenum and downcomer is boiling off, going up through the pressurizer and out the open RVVs to containment. Around the time the core starts to heat up at 8.7 hours, a flow pattern begins with steam flow going from the heating core, up the riser, turning around at the PZR baffle plate, down the downcomer, and back into the riser through a bypass flowpath at the 3 meter elevation. The flow rate appears to provide enough cooling to the riser and core that the collapse of the remainder of the lower nodes of ring one is delayed by several hours as can be seen in Figure 3.7 as well as the subsequent failure of ring 2 being delayed. During the audit beginning March 6, 2018 (Reference 11), the applicant stated that this bypass flowpath has been removed from the NuScale design and does not exist in the applicant's MELCOR deck. Hence, in the applicant's analysis, flow from the downcomer to the core only occurs after the

[redacted]

downcomer water level falls below the support plate. The applicant's predicted SG pressure rise at [redacted] hours is due to the water level going below the lower core support plate and this natural circulation beginning. Two sensitivity calculations are given in Section 4 for scenarios LEC-06T and LCC-05T with this bypass flowpath removed from the staff's deck. The removal had little impact on the LCC-05T calculation, but did have an impact on event times in the LEC-06T calculation.

Between 10.6 and 17.6 hours, the bottom two nodes of ring one and the bottom four nodes (out of 6) of ring two are still upright. At 17.6 hours, the RPV water level drops below the BAF. The core heats up due to core uncovery and ongoing oxidation of the zircaloy cladding. The remaining upright portion of ring 1 heats up over the following hour and collapses at 18.5 hours with the remaining upright portion of ring 2 collapsing a few minutes later. With debris accumulating on the core support plate, it heats up leading to its failure in rings 1 and 2 fail at 19.5 and 20.7 hours, respectively. At the end of the staff's simulation (as of 48 hours), ring 3 remains upright and rings 1 and 2 are a rubble bed sitting in the lower plenum and lower core region. Prior to a deck correction (water elevation in one of the RPV control volumes was corrected leading to additional water inventory in the RPV), this same scenario led to the core support plate of the outermost ring failing very late in the accident (47 hours) and ring 3 collapsing into rubble. Hence, there is some uncertainty associated with the timing and extent of core failure.

The release fraction of fission products from the fuel is shown in Figure 3.10 with the airborne fraction in containment given in Figure 3.11.

[redacted]

[redacted]

Table 3.1 A comparison of event timings in simulation LEC-06T for both the staff and applicant's MELCOR calculations.

LEC-06T		
Event	**Time (seconds)**	
	Applicant	**Staff**
RVV LOCA	0	0
CNV Isolation signal	0	0
SCRAM	2	2
IAB cleared	**	11
Maximum CNV pressure	40	70
ECCS signal on low RPV level	**	2213
Partial ECCS actuation	1010	2213
ECCS signal on high CNV level	1010	4617
PZR heater isolation*	1432	0
Low low PZR level (20%)	2319	1380
RPV collapsed level below TAF	16200 (4.5hr)	19000 (5.3 hr)
High core outlet temperature (610F)	21973 (6.1hr)	30400 (8.4 hr)
Onset of cladding oxidation	24360 (6.8hr)	31259 (8.7 hr)
Gap release in ring 1	24539 (6.8hr)	31542 (8.8 hr)
Core damage (PCT>2200F)	25223 (7hr)	32600 (9.1 hr)
Gap release in ring 2	**	32889 (9.1 hr)
Gap release in ring 3	**	35171 (9.8 hr)
Maximum cladding temperature	29640 (8.2hr)	35560 (9.9 hr)
RPV collapsed level below BAF	**	63400 (17.6 hr)
Failure of core support plate (ring 1)	41785 (11.6hr)	70033 (19.5 hr)
Failure of core support plate (ring 2)	**	74559 (20.7 hr)
End of cladding oxidation	95400 (26.5hr)	104100 (28.9 hr)
End of simulation	259200 (72hr)	172800 (48 hr)

*In the staff's MELCOR model, the PZR heater is not explicitly modeled. Instead a control function is used during the steady state to add enthalpy to the pressurizer. When the steady-state calculation is complete (at time 0), the enthalpy addition is assumed to end.
**Data not available.

[redacted]

[redacted]

Figure 3.1 LEC-06T: Short-term pressure in the CNV, RPV and SGs.

Figure 3.2 LEC-06T: Long-term pressure in the CNV, RPV and SGs.

[redacted]

[redacted]

Figure 3.3 LEC-06T: Total core power.

Figure 3.4 LEC-06T: Collapsed liquid level in the RPV, CNV and steam generators.

[redacted]

[redacted]

Figure 3.5 LEC-06T: Integrated mass flowing through the ECCS valves. Note that the RVV #2 and #3 curves are identical.

Figure 3.6 LEC-06T: Mass balance of water in the CNV, RPV and steam generators. Note that the SG water mass is on the secondary vertical axis for viewing convenience.

[redacted]

[redacted]

Figure 3.7 LEC-06T: Cladding temperatures of ring 1 of the core for each node (node 5 being the lowest and node 11 being the highest).

Figure 3.8 LEC-06T: Cladding temperatures of upper fuel elevation (5th highest of 6 axially stacked fuel nodes) for each ring and the peak cladding temperature of all fuel nodes.

[redacted]

[redacted]

Figure 3.9 LEC-06T: Hydrogen generated.

Figure 3.10 LEC-06T: Fraction of radionuclide inventory released from the fuel.

[redacted]

[redacted]

Figure 3.11 LEC-06T: Fraction of the radionuclide inventory airborne in containment.

[redacted]

3.2. LCC-05T

This scenario, referred to as LCC-05T in the applicant's FSAR, is initiated by a break in the CVCS line at elevation [redacted] ft, inside of containment. Due to an oversight, the staff's MELCOR simulation has the break at 13 meters (42.7 ft.) which is near the pressurizer baffle plate. A sensitivity calculation is performed in Section 4 with the break location corrected to [redacted] feet and shows little impact on the results of the simulation. Upon ECCS actuation and after the IAB allows ECCS valves to open, there is a partial failure (all three RVVs open and both RRVs remain closed). The DHRS is assumed to be unavailable.

A summary of the event timings is given in Table 3.2. Figure 3.12 through compare the simulation results of the staff and applicant. In the following discussion, the numbers cited are for the staff's MELCOR simulations unless otherwise stated.

Figure 3.12 gives the pressure in the RPV, CNV and SGs (the two SGs are identical and conditions within are also identical) in the first 30 minutes of the accident. As stated before, the initiating event is a break in the CVCS line into containment. The CVCS line break is a [redacted] in^2 pathway from a location above the top of the core in the riser (CV174 in Figure 2.1) to the space between the RPV and CNV (CV413 in Figure 2.2). As a result of the break, the RPV and SG pressures decrease. ECCS actuates and the RVVs open on low RPV level at 790 seconds. As steam condenses on the CNV wall, pressure in the CNV and RPV decreases. In the staff's calculations both here and in LEC-06T, the SG pressure follows RPV pressure until the water level falls below the bottom of the SGs (see Figure 3.13). This is not seen as significantly in the applicant's calculation. This was discussed with the applicant during the March 2018 audit. (See discussion in the LEC-06T section above).

The long-term pressure is given in Figure 3.13. As mentioned in the LEC-06T discussion, the staff's MELCOR deck included a bypass flowpath that allows a recirculatory flow pattern to begin early on (around 2.6 hours) and increase the heat transfer to the SG tubes and cause a gradual increase in SG pressure. It also provides cooling to the area above the core. This bypass flowpath is not a part of the current NuScale design and was therefore not a part of the applicant's MELCOR model. Hence, a flow from the downcomer to the core region only occurs in the applicant's calculation when the RPV downcomer water level falls below the core support plate. In the applicant's calculation, then, SG temperature and pressure rises more rapidly and at a later time (around [redacted] hours). Section 4.5 describes a sensitivity calculation of the staff's LCC-05T calculation without the bypass flowpath included (see discussion in the LEC-06T section above). However, staff were still unable to replicate the sharp depressurization of the SG seen in the applicant's calculations.

Water levels are given in Figure 3.14 and Figure 3.15. The water levels are similar between the staff's and applicant's MELCOR simulations. Figure 3.18 shows that the mass of water in the RPV, CNV, and SGs for the staff and applicant's simulations has good long term agreement regardless of the differences in the RVV modeling.

Following core uncovery, core heat up and degradation occurs (see Figure 3.19). Cladding oxidation begins at 3.4 hours and gap release in ring one of the core occurs at 3.5 hours. Recall that in the staff's deck, the core is nodalized as three radial rings with 9, 14, and 14 assemblies respectively while the licensee's deck is nodalized as four radial rings with [redacted]

assemblies. In the staff's simulation, the upper levels of the ring 1 heat up and collapse at 4.4 hours. The downward relocation of core debris into the water generates steam which temporarily cools the core. The remainder of ring 1 collapses 2 hours later along with all of ring 2 after the water level has fallen below the BAF. Ring three is much slower to heat up since it has heat transfer to the heavy reflector and CNV vessel and collapses at 16.7 hours.

There is more hydrogen generated in the applicant's simulation as seen in Figure 3.20. In the applicant's simulation, the two inner rings of the core remain upright for a greater period of time and the remaining two rings remain upright indefinitely. This allows for more interaction of steam with the zircaloy cladding and thereby hydrogen generation. In contrast, in the staff's simulation, rings one and two collapse before 8 hours and the outermost ring collapses around 16 hours. Around 8 hours, hydrogen generation slows and at 16 hours, it has ceased.

The release fraction of fission products from the fuel is shown in Figure 3.21 with the airborne fraction in containment given in Figure 3.22.

Table 3.2 A comparison of event timings in simulation LCC-05T for both the staff and applicant's MELCOR calculations.

LCC-05T		
Event	**Timing (seconds)**	
	Applicant	**Staff**
CVCS LOCA	0	0
SCRAM	3	3
PZR heater isolation*	40	3
Low low PZR level (20%)	90	240
ECCS signal on low RPV level	**	790
IAB cleared	**	900
Maximum CNV pressure	700	900
ECCS signal on high CNV level	681	915
RPV collapsed level below TAF	7860 (2.2hr)	7720 (2.2 hr)
High core outlet temperature (610F)	14625 (4.1hr)	10600 (2.9 hr)
Onset of cladding oxidation	16440 (4.6hr)	12179 (3.4 hr)
First gap release (ring 1)	16593 (4.6hr)	12424 (3.5 hr)
Core damage (PCT>2200F)	17190 (4.8hr)	13260 (3.7 hr)
Gap release in ring 2	**	13835 (3.8 hr)
Gap release in ring 3	**	15417 (4.3 hr)
Maximum cladding temperature	21120 (5.9hr)	16260 (4.5 hr)
RPV collapsed level below BAF	**	19644 (5.5 hr)
Failure of core support plate (ring 1)	33963 (9.4hr)	29146 (8.1 hr)
Failure of core support plate (ring 2)	**	37085 (10.3 hr)
Failure of core support plate (ring 3)	**	60206 (16.7 hr)
End of cladding oxidation	150000 (41.7hr)	continues
End of simulation	259200 (72hr)	172800 (48 hr)

*In the staff's MELCOR model, the PZR heater is not directly modeled. Instead a control function is used during the steady state to add enthalpy to the pressurizer. When the reactor SCRAMs, the control function ceases.
**Data not available.

[redacted]

Figure 3.12 LCC-05T: Short-term pressure in the CNV, RPV and SGs.

Figure 3.13 LCC-05T: Long-term pressure in the CNV, RPV and SGs.

[redacted]

[redacted]

Figure 3.14 LCC-05T: Short-term swollen liquid level in the RPV, CNV and SGs.

Figure 3.15 LCC-05T: Long-term swollen liquid level in the RPV, CNV and SGs.

[redacted]

[redacted]

Figure 3.16 LCC-05T: Integrated mass flowing through the ECCS valves. Note that the three RVV curves are superimposed.

Figure 3.17 LCC-05T: Integrated mass flowing through the CVCS break.

[redacted]

[redacted]

Figure 3.18 LCC-05T: Mass balance of water in the CNV, RPV and steam generators.

Figure 3.19 LCC-05T: Cladding temperatures of upper fuel elevation (5th highest of 6 axially stacked fuel nodes) for each ring and the peak cladding temperature of all fuel nodes.

[redacted]

[redacted]

Figure 3.20 LCC-05T: Hydrogen generated.

Figure 3.21 LCC-05T: Fraction of the core inventory released from the fuel.

[redacted]

[redacted]

Figure 3.22 LCC-05T: Fraction of the core inventory airborne in containment.

[redacted]

[redacted]

3.3. LCU-03T

This scenario, referred to as LCU-03T in the applicant's FSAR, is initiated by a break in the CVCS line at elevation [redacted] ft., outside of containment (CV518 in Figure 2.3). ECCS is assumed not to actuate and the DHRS is assumed unavailable. Feedwater injection is assumed to end at the time of reactor SCRAM.

A summary of the event timings is given in Table 3.3. Figure 3.23 through Figure 3.31 compare the simulation results of the staff and applicant. In the following discussion, the numbers cited are for the staff's MELCOR simulations unless otherwise stated.

The staff's results reported in this section terminated a few hours after RPV lower head failure and corium relocation to the containment lower head. The cause of the termination was determined to be an issue with MELCOR's new containment lower head model which becomes active following corium relocation to the containment lower head. By this time, in-vessel core-melt progression has ended and because this is a bypass event, the staff decided that additional effort on this confirmatory analysis was not cost beneficial.[2]

Figure 3.23 gives the pressure in the RPV, CNV and SG in the first 30 minutes of the accident. As stated before, the initiating event is a break in the CVCS line outside of containment. Since this is a bypass accident, CNV pressure remains constant at 0 psia. Because it is a break of the CVCS injection line, water comes out of the break until the RPV water level decreases to the bottom of the CVCS line. As a result, Figure 3.23 shows that the RPV pressure is steady for the first 30 minutes of the accident. Figure 3.24 shows the longer-term RPV pressure reduction as a result of the CVCS line break outside containment.

The water level in the RPV, CNV and SGs is given in Figure 3.25 and Figure 3.26. RPV water is lost through the CVCS break. As is seen in Figure 3.27 the leak rate of the CVCS break is greater in the applicant's analysis than in the staff's resulting in core uncovery occurring an hour sooner in the applicant's analysis.

Figure 3.28 gives the water inventory of the RPV, CNV, and SGs. Since this is a bypass event, water that is lost from the RPV does not make its way into containment. The 1200 kg of water that appears in the CNV around 6 hours is from the SG relief valve opening into containment. Figure 3.29 provides the temperature of the uppermost elevation of the core for each ring. The temperature going to zero indicates the fuel in the cell is no longer intact (formation of debris). By 10.2 hours, all three rings of the lower core plate have failed resulting in downward relocation of the core into the lower plenum. Figure 3.30 gives the hydrogen generated by the zircaloy/steam reaction and Figure 3.31 gives the release fraction of volatile fission products from the fuel.

[2] Following completion of this analysis, the code error was corrected an a rerun of this sequence with the new code version showed that there are some differences in the results following core damage, but well within uncertainties one would expect from a severe core damage accident.

[redacted]

[redacted]

Table 3.3 Comparison of event timing for both NuScale and NRC staff's MELCOR calculations of LCU-03T

LCU-03T		
Event	**Timing (seconds)**	
	Applicant	**Staff**
CVCS LOCA	0	0
SCRAM on low PZR level (<35%)	69	69
Low PZR pressure	87	488
Low low PZR level (20%)	92	700
ECCS signal on low RPV level	1259	2269
IAB cleared	**	6380 (1.8 hr)
RPV collapsed level below TAF	4572 (1.3 hr)	7840 (2.2 hr)
Onset of cladding oxidation	8760 (2.4 hr)	13698 (3.8 hr)
Gap release in ring 1	8942 (2.5 hr)	14010 (3.9 hr)
Core damage (PCT<2200F)	9493 (2.6 hr)	15020 (4.2 hr)
Maximum cladding temperature	11640 (3.2 hr)	15220 (4.2 hr)
Gap release in ring 2	**	15227 (4.2 hr)
Gap release in ring 3	**	16662 (4.6 hr)
RPV collapsed level below BAF	**	16754 (4.7 hr)
Failure of core support plate (ring 1)	18110 (5.0 hr)	22887 (6.4 hr)
Failure of core support plate (ring 2)	**	31728 (8.8 hr)
Failure of core support plate (ring 3)	**	36748 (10.2 hr)
Relief valve opens allowing water to CNV	19800 (5.5 hr)	20240 (5.6 hr)
Failure of RPV lower head	42220 (11.7 hr)	57070 (15.9 hr)
End of cladding oxidation	63480 (17.6 hr)	continues
End of simulation	259200 (72 hr)	*

*Staff's MELCOR calculation terminated after failure of RPV lower head.
**Data not available.

[redacted]

[redacted]


[redacted]

Figure 3.23 LCU-03T: Short-term pressure in the CNV, RPV and SGs.


[redacted]

Figure 3.24 LCU-03T: Long-term pressure in the CNV, RPV and SGs.

[redacted]

[redacted]

Figure 3.25 LCU-03T: Short-term swollen liquid level in the RPV, CNV and SGs.

Figure 3.26 LCU-03T: Long-term swollen liquid level in the RPV, CNV and SGs.

[redacted]

[redacted]

Figure 3.27 LCU-03T: Integrated mass flowing through the CVCS break.

Figure 3.28 LCU-03T: Mass balance of water in the CNV, RPV and SGs. The vendor's SG mass does not include water in the feed and steam lines while the staff's does.

[redacted]

Figure 3.29 LCU-03T: Cladding temperatures of upper fuel elevations for the three rings and the peak cladding temperature.

Figure 3.30 LCU-03T: Hydrogen generated.

[redacted]

Figure 3.31 LCU-03T: Mass fraction released in-vessel.

[redacted]

4. Sensitivity Calculations to MELCOR Calculations

4.1. RVV Flow Area

This scenario is a sensitivity calculation based on LEC-06T.

As noted above, the RVV flow areas are different between the staff and applicant's decks. The staff requested (as part of the 2017 PRA and SA Audit (Reference 12) from NuScale the "best estimate" flow area of the RVVs and found that it had changed since the applicant had performed their MELCOR calculations for FSAR Revision 0. This more recent value was used in the staff's calculations documented in Section 3.1. As a result, the RVV flow area used in the staff's deck is smaller than that of the applicant (1.119E-2 m^2 versus [redacted] m^2 per valve). The staff ran this sensitivity calculation of with a flow area of [redacted] m^2 per valve to test the significance of this difference and whether the RVV flow area contributes to core uncovery occurring about an hour later in the staff's calculations (see Table 3.1).

Results of the sensitivity calculation are shown in Figure 4.1 through Figure 4.3. As indicated by the figures, the larger RVV flow area does not appear to have much of an impact on the results of the scenario and does not account for the observed differences in the staff and applicant's results. The pressure in the RPV and CNV in the first few minutes of the simulation is still higher in the staff's results than the applicant's; the integrated flow through the open RVVs is the same as the base calculation; and the uncovering of the core occurs at roughly the same time as the base calculation.

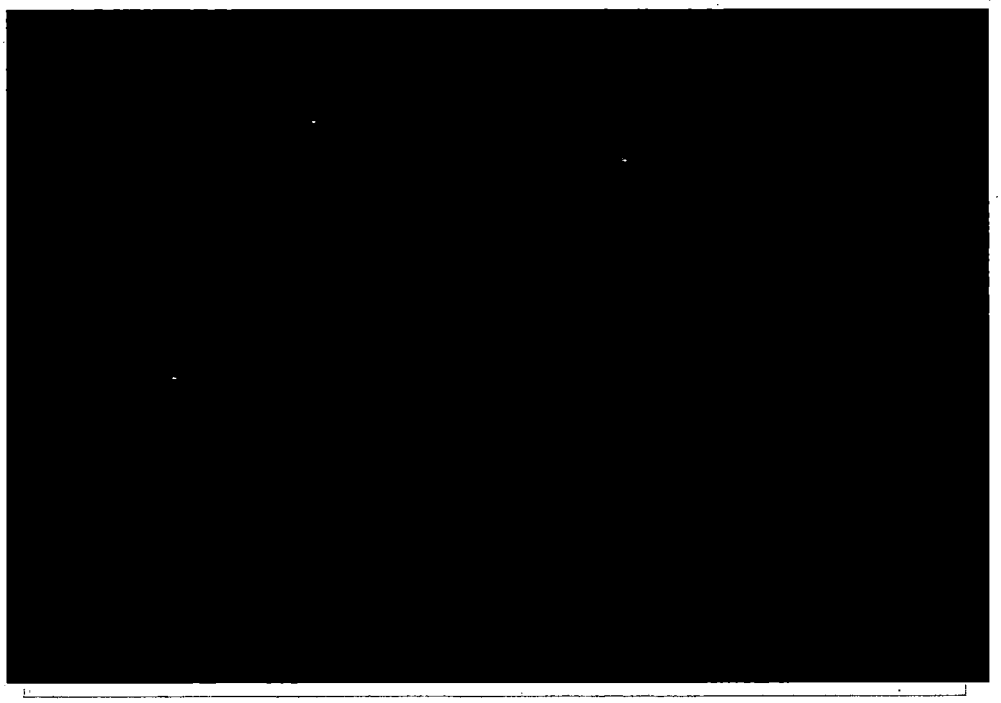

Figure 4.1 LEC-06T: Absolute pressure in the CNV, RPV and steam generators (detailed).

[redacted]

Figure 4.2 LEC-06T: Integrated mass flowing through the ECCS RVVs for the staff's base and sensitivity cases and vendor's case.

Figure 4.3 LEC-06T: Collapsed liquid level in the RPV and CNV for the staff's base and sensitivity cases and vendor's case.

[redacted]

[redacted]

4.2. SG Nodalization

This scenario is a sensitivity calculation based on LEC-06T.

The steam generator nodalization with four axial levels used in the staff's deck (see Figure 2.1) uses fewer volumes than the applicant. A consequence of the bottommost node being so large in the base model was that the heat transfer modeled in the steam generators was coarse and led to an increased overall RCS temperature in the steady-state. For this sensitivity, the topmost node and bottommost nodes of both SGs were split into three vertically stacked nodes and staff then ran LEC-06T with this modified nodalization.

Figure 4.4 shows that, with the finer nodalization, there was improved agreement between the staff and the applicant's pressures in the first few minutes following the start of the accident.

In the longer-term, Figure 4.5 shows that the SG pressure in the sensitivity case is the same as the base case up to the time where the RPV water level falls below the TAF and the recirculation flow discussed in Section 3.1 begins. Beyond this time, the pressure difference in the base and sensitivity calculations may come from the difference in initial SG water inventory. With the finer nodalization, the initial conditions in the SGs are slightly different for the sensitivity. The initial (swollen) water level in the SGs is higher (12.3m versus 10.5m).

The RPV and CNV water levels are given in Figure 4.6. The flow rate through the open RVVs is reduced and the rate of inventory loss is slowed.

Figure 4.4 LEC-06T: Comparison of short-term pressure in the RPV, CNV, and SGs.

[redacted]

[redacted]

Figure 4.5 LEC-06T: Comparison of long-term pressure in the RPV, CNV, and SGs.

Figure 4.6 LEC-06T: Comparison of collapsed water level in the RPV, CNV, and SGs.

[redacted]

[redacted]

4.3. Timing of ECCS Actuation

This scenario is a sensitivity calculation based on LEC-06T.

There was a difference in timing for ECCS valve opening in the staff and applicant's calculations. It stems from a change in the applicant's ECCS actuation setpoint on CNV actuation level. The applicant changed their ECCS actuation setpoint after they completed their MELCOR analysis. Because of this change, the staff's calculations used a higher level for ECCS actuation than the applicant's calculations and, as a result, the 2nd and 3rd RVVs opened at 1,010s versus the staff's 2,213s. A sensitivity calculation of LEC-06T was therefore performed to test the significance of this difference and whether the timing in ECCS actuation contributes to the core uncovering an hour later in the staff's calculations than in the applicant's. The deck was modified to force ECCS valves to open at 1,010s to match the applicant's simulation.

This sensitivity resulted in a shift in the integrated flow through the RRVs. Figure 4.7 compares the integrated flow through the RVVs for the staff's two calculations to the applicant's calculation. The flow through the first RVV (RVV1) is significantly less and the other two valves discharge more volume. In the end, however, the decreased flow through the first valve is compensated for by the increased flow through the other two. Figure 4.8 demonstrates that there is no impact on the staff's predictions of RPV level and the timing of core uncovery. In Figure 4.8, the RPV-staff line covers the RPV-sens line.

Figure 4.7 LEC-06T: Integrated mass flowing through the RVVs. Note that RVVs 2 and 3 are identical.

[redacted]

[redacted]

Figure 4.8 LEC-06T: Collapsed liquid level in the RPV and CNV.

[redacted]

[redacted]

4.4. CVCS Break Location

This scenario is a sensitivity calculation based on LCC-05T.

In the staff's deck, the CVCS break inside containment was modeled as a flowpath with one end in the riser just above the core and the other end inside containment at elevation [redacted] meters which is near the elevation of the RPV pressurizer baffle plate. However, the applicant assumed that this flowpath ended in containment at [redacted] meters which is at the top of containment. The applicant made this assumption to prevent liquid water from re-entering the RPV. Therefore, the staff performed a sensitivity calculation changing the break location to [redacted] meters to assess the impact of this difference.

The sensitivity calculation predicts that the ECCS signal on low RPV level occurs at the same time as the base case (790 s). However, as Figure 4.9 shows, the sensitivity case has a slightly lower pressure in the CNV than in the base case. The IAB – which prevents the ECCS valves from opening if the differential pressure between RPV and CNV is greater than 1000 psi-d – clears two and a half minutes later in this sensitivity case as compared to the base case. This leads to an increased loss of RPV water inventory through the CVCS break and a decreased loss through the RVVs (see Figure 4.12 and Figure 4.13). The overall effect is that core uncovery occurs sooner and core oxidation begins at 2.8 hours in the sensitivity rather than at 3.4 hours in the base case (see Figure 4.10 and Figure 4.11). Figure 4.11 shows that the containment water level does not exceed the break elevation in either the [redacted]-meter of the [redacted] meter break. There is a shift in timings in this sensitivity due to the delayed opening of the RVVs. For example, core oxidation starts 24 minutes sooner, RPV level is below BAF 1.1 hours sooner, and ring one of the core support plate fails 2 hours earlier.

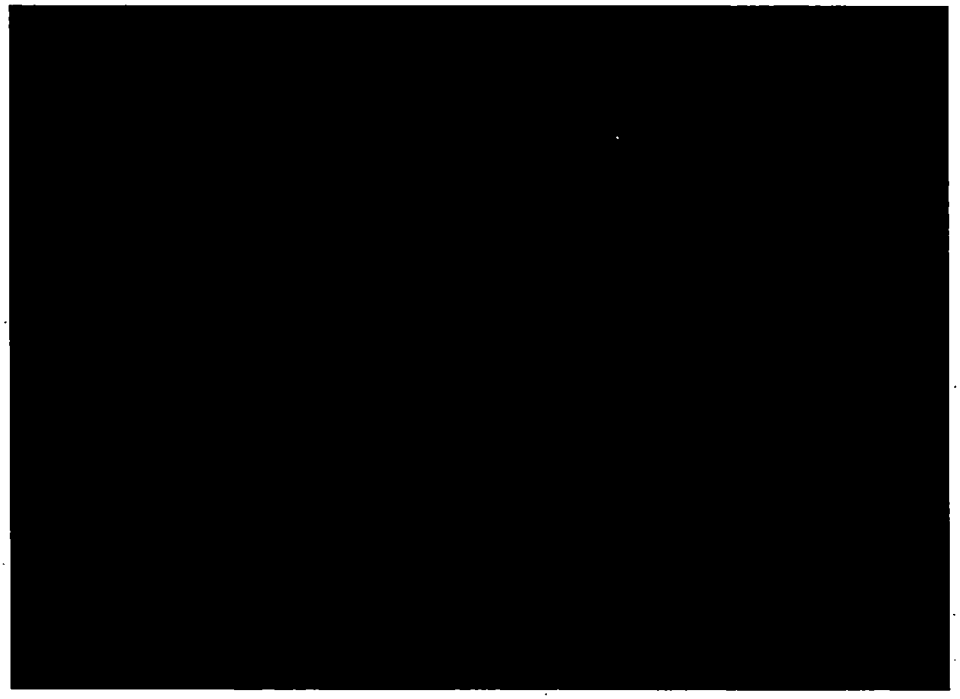

Figure 4.9 LCC-05T: Short-term pressure in the CNV, RPV and SGs.

[redacted]

[redacted]


[redacted]

Figure 4.10 LCC-05T: Short-term collapsed liquid level in the RPV and CNV.


[redacted]

Figure 4.11 LCC-05T: Long-term collapsed liquid level in the RPV and CNV.

[redacted]

[redacted]

Figure 4.12 LCC-05T: Integrated mass flowing through the CVCS break.

Figure 4.13 LCC-05T: Integrated mass flowing through the ECCS valves. Note that the three RVV curves are identical.

[redacted]

[redacted]

4.5. Removal of the Bypass Flowpath Between Downcomer and Riser

As a result of discussions during an audit beginning March 6, 2018 (Reference 11), the staff found that a [redacted] m^2 area bypass flowpath going from the downcomer (CV110 in Figure 2.1) to the area inside the riser just above the core (CV in Figure 2.1) was eliminated from the NuScale design in 2015. Therefore, the staff ran two sensitivity calculations below (one for LEC-06T and one for LCC-05T) to assess the impact of its removal.

LEC-06T

As described in Section 3.1, during a severe accident the bypass flowpath allows a small amount of vapor flow from the RPV downcomer to the riser creating a recirculatory flow of gas in the RPV before the lower core plate is uncovered. The case with bypass flow predicts lower core plate failure for rings 1 and 2 at 18 hours, while the case without bypass flow predicts lower core plate failure at 13 hours see Figure 3.7 and Figure 4.15). Comparing Figure 3.7 with Figure 4.15 demonstrates this extended time to failure of the bottommost nodes of ring one in the base case.

While the fuel collapses in ring one collapses at 13 hours, the core support plate for ring one fails at 15 hours which accelerates the loss of water inventory. The water level in the downcomer region falls below the lower core plate around 16.5 hours and flow from the downcomer, through the rubble bed in the lower plenum, through the core region and up the hot leg riser begins. When this pattern is established, hot vapor flows over the SG tubes and the water within the tubes heats up. Pressure in the SGs increases more quickly than in the staff's base case (see Figure 3.2), though still not as quickly as in the applicant's case as shown in Figure 4.14. Also, the sensitivity case has an increased flow of steam over the upright third ring of the core. The lower core plate of ring 3 fails at 23.4 hours which is in contrast to the original calculation where the lower core plate of ring 3 does not fail. As a result, there is a higher release fraction of fission products in this case with ring 3 heating up as a rubble bed.

In summary, core degradation progresses more quickly in the sensitivity calculation. Failure of the core support plate occurs at 15, 17 and 23 hours for rings 1, 2, and 3, respectively. With the core support plate under all three rings failing in this case, the rubble bed in the lower plenum is larger and heats up more and the release fraction from the fuel is greater (as seen in Figure 4.16).

[redacted]

[redacted]


[redacted]

Figure 4.14 LEC-06T: Pressure in the RPV, CNV, and SGs.

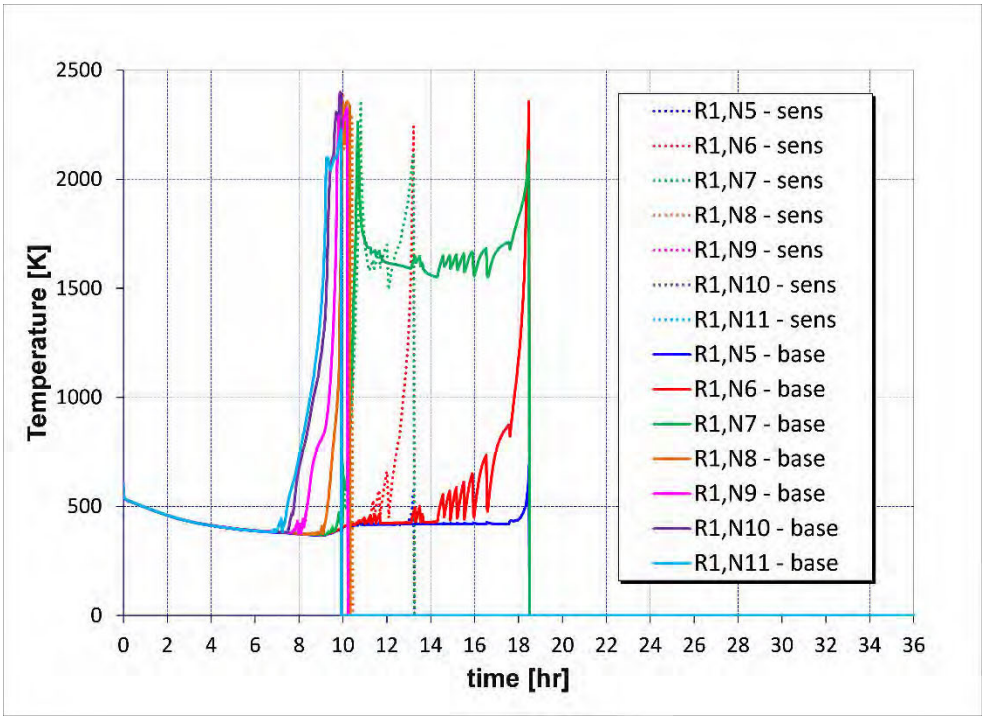

Figure 4.15 LEC-06T: Cladding temperatures of ring 1 of the core for each node (node 5 being the lowest and node 11 being the highest).

[redacted]

[redacted]

Figure 4.16 LEC-06T: Fraction of radionuclide inventory released from the fuel.

[redacted]

[redacted]

LCC-05T

Without the bypass flowpath, the circulatory vapor flow pattern does not start from the downcomer to the core region until water level falls below the lower core plate at 8 hours. However, the timing of events is very similar to the base case (see Figure 4.17, Figure 4.18, and Figure 4.19). Figure 4.20 which compares the vapor temperatures in the staff's base and sensitivity cases reveals that there is little difference in the results. Without the flowpath, there is complete ring one collapse 17 minutes sooner and ring two collapse 15 minutes sooner.

Eliminating the bypass flowpath for LCC-05T (CVCS LOCA) affects the results less than eliminating the bypass flowpath for LEC-06T (RVV LOCA). This could be due to more rapid time to core uncovery and damage for LCC-05T (CVCS LOCA). Also, the release fractions are the same for the LCC-05T base and sensitivity cases.

Figure 4.17 Pressure in SG 1, RPV and CNV for the staff's sensitivity case and the vendor's calculation.

[redacted]

Figure 4.18 Release fractions from the fuel for the staff's sensitivity case and the vendor's calculation.

Figure 4.19 Water level in the RPV and CNV for the staff's sensitivity case and the vendor's calculation.

[redacted]

[redacted]

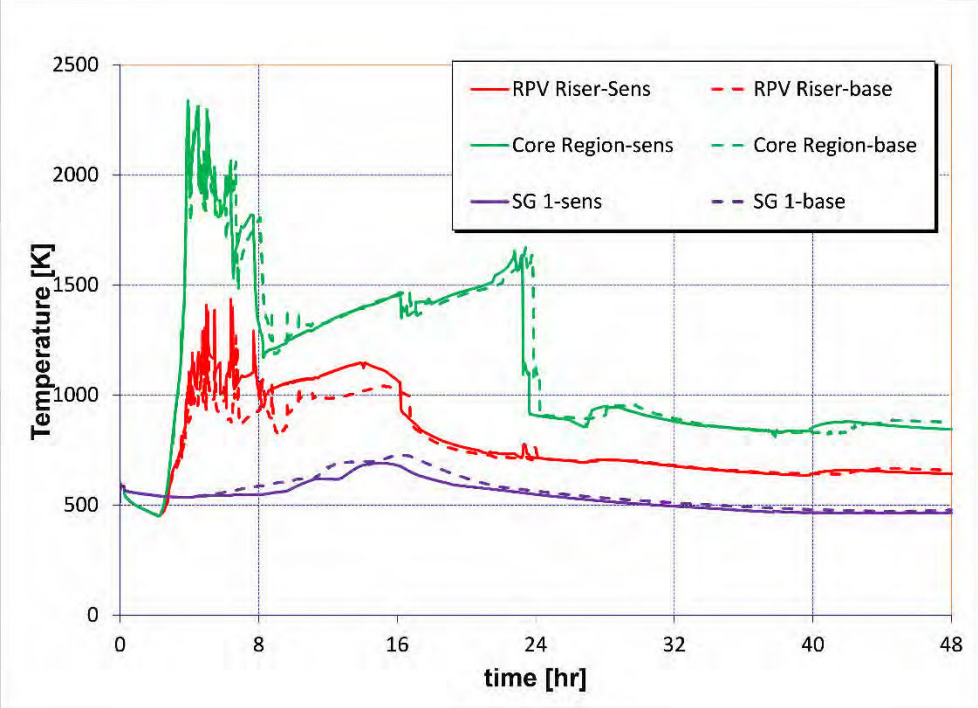

Figure 4.20 Vapor temperatures in the RPV riser, SG 1, and Core region for the staff's sensitivity and base cases.

[redacted]

[redacted]

5. Confirmatory Analysis for the NuScale Accident Source Term Topical Report

5.1. Introduction

The NuScale Accident Source Term Methodology Topical Report (Reference 5) provides a method for estimating the EAB, LPZ and control room doses. It also includes a sample analysis of EAB, LPZ and control room doses which is referenced in the FSAR. The topical report covers the source term from the RPV to the containment, the in-containment aerosol removal rate, and containment leak rate. The staff's independent confirmatory analysis performed in support of its review of the topical report is described below. Section 5.2 assesses the source term from the RPV to the containment. Section 5.3 assesses the in-containment aerosol removal rate. Section 5.4 assesses containment leak rate. Section 5.5 assesses the release from the containment to the environment.

The results of the MELCOR base case calculation in Section 3.1 for RVV LOCA (LEC-06T) is used for the staff's independent assessment of the topical report. LEC-06T is initiated by the spurious opening of a single RVV followed by partial actuation of the ECCS (the remaining two RVVs open and both RRVs remain closed). The DHRS is assumed unavailable in this scenario. The timing of key events for LEC-06T is compared between the applicant's and staff's MELCOR calculations in Table 3.1.

5.2. Source Term from the RPV to Containment

In the topical report, the release fraction of fission products to containment for the representative source term is determined by taking the median release from four MELCOR calculations based on an earlier version of the NuScale design. The applicant subsequently performed five MELCOR calculations based on the final version of the NuScale design (as described in FSAR Revision 0 and underlying documentation) to confirm the analysis. Table 5.1 shows the results of the five MELCOR calculations based on the final version of the design and also the results of the staff's MELCOR results for LEC-06T.

The topical report states that the release durations into containment are estimated as the time when 90% of the volatile fission products that reach the containment by the end of the accident have entered the containment. The topical report does not state which fission product group (e.g., iodine, cesium) is used for this metric. In the staff's MELCOR simulation, 90% of the iodine enters containment by 19.5 hours while 90% of the cesium enters containment by 18.5 hours for a duration of either 10.7 or 9.7 hours. For the staff's comparison, the former is chosen since iodine is typically the dominant contributor to EAB, LPZ, and control room doses.

The second through sixth columns of Table 5.1 give the applicant's cumulative release fractions into containment for the five MELCOR calculations based on the final version of the NuScale design. The ninth column of Table 5.1 gives the staff's cumulative release fraction into the containment of noble gases, iodine, and cesium at the end of 48 hours. The fraction of core inventory of volatile fission products in containment is given in Figure 5.1 . The curve for noble gases is not flat but reaches a relative peak value of 0.55 before decreasing again due to flow back into the RPV. Similar behavior is not seen for iodine and cesium, because these are in aerosol form and deposit in the containment so cannot flow back into the RPV through the open RVVs. Table 5.1 lists this peak value for the release fraction of noble gases into containment.

[redacted]

[redacted]

Figure 5.2 gives the release fraction of iodine that is released from the core and present in the RPV and containment.

Table 5.1 Release fractions and time of the five representative accident scenarios from the applicant's MELCOR calculations (Reference 13) as compared to the Staff's MELCOR result. DHRS was available in all scenarios until core damage.

		Case 1	Case 2	Case 3	Case 4	Case 5	Median	Reg. Guide 1.183	NRC Staff (LEC-06T)
		CVCS break, no ECCS	CVCS break, RRVs open	CVCS break, RVVs open	RRVs open	RVVs open	Repres-entative Source Term[1]	PWR DBA LOCA	RVVs open
Start of gap (hrs)		17.6	3.8	8.1	6.2	21.3	3.8	30 sec	8.8
Release duration (hrs)		12.0	1.0	9.0	1.3	14.0	1.0	1.8	10.7
Release fraction	NG	0.39	0.19	0.41	0.19	0.48	0.39	1.0	0.55
	I	0.21	0.035	0.16	0.019	0.14	0.14	0.4	0.18
	Cs	0.25	0.059	0.22	0.031	0.20	0.20	0.3	0.29

[1]The representative source term per the topical report methodology uses the shortest time for the start of release and the release duration. It then uses the median release fractions.

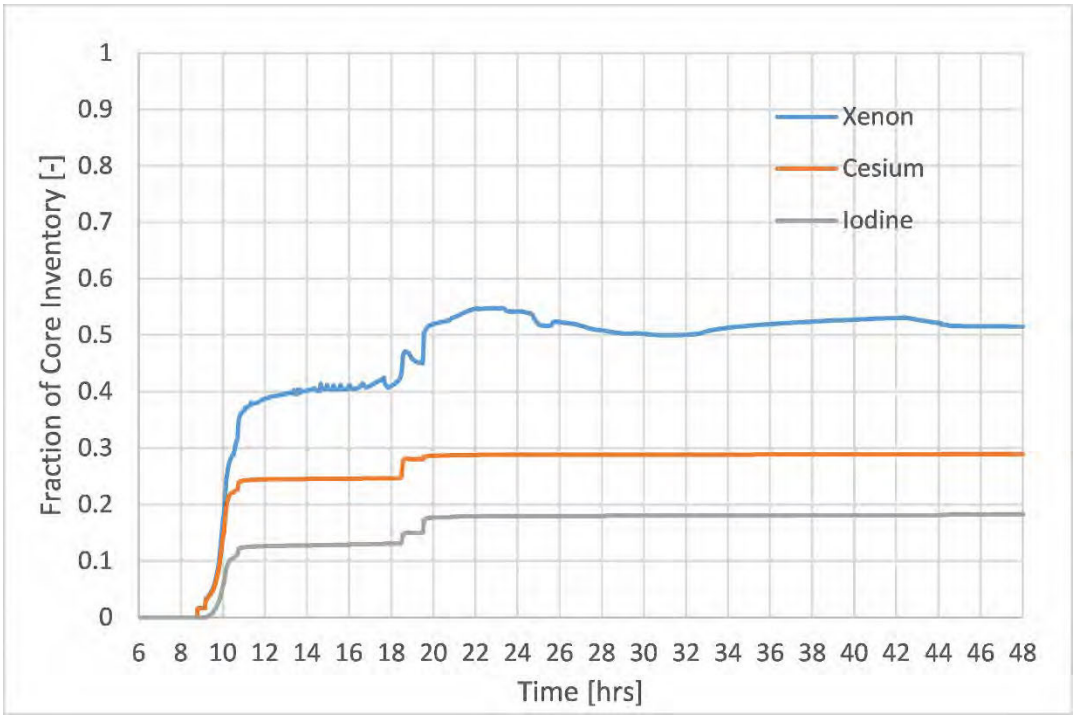

Figure 5.1 LEC-06T: Radionuclide inventory in containment as a fraction of total core inventory.

[redacted]

[redacted]

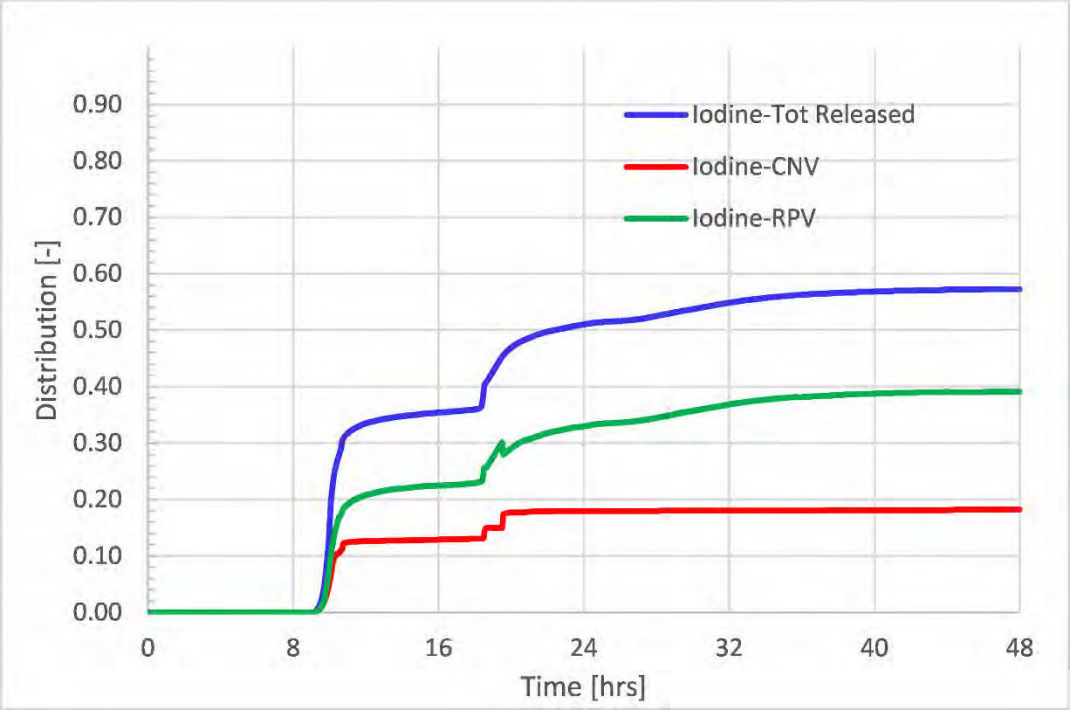

Figure 5.2 LEC-06T: Distribution of iodine in containment as a fraction of total core inventory.

5.3. In-containment Aerosol Removal Rate

The NuScale accident source term methodology topical report describes a number of removal mechanisms and uses the STARNAUA code (with thermal hydraulic input from the applicant's MELCOR simulations) to calculate the gravitational settling removal rate of airborne aerosols in the containment.

Figure 5.3 shows the airborne aerosol concentration and removal rate that is provided in the applicant's Accident Source Term Topical Report for an example source term calculation (Figure 5-13 of the topical report). Staff identified two issues with this figure. First, the airborne concentration is reported in g/cm^3 which is unrealistically high. Second, the applicant's aerosol removal rate increases linearly as the aerosol concentration decreases. As the airborne concentration decreases, the likelihood of agglomeration should also decreases and the deposition rate should slow.

Below, the staff used the results of its MELCOR simulation for LEC-06T to assess the aerosol removal rates that the applicant calculated with STARNAUA. MELCOR models removal of airborne fission products through Brownian diffusion, gravitational settling, thermophoresis, and diffusiophoresis. While the applicant only modeled gravitational settling/agglomeration, the staff included all available aerosol removal mechanisms in MELCOR. Below, the staff's MELCOR prediction of the concentration of airborne versus deposited aerosols is used to estimate a removal rate for containment to be compared to the applicant's.

The concentration of airborne fission products in containment is given by the equation

[redacted]

[redacted]

$$\frac{dC}{dt} = -\lambda(t) \cdot C(t) + \frac{dS}{dt}$$

where,

$C(t)$ is the concentration of airborne aerosols in the containment at time t (g/m^3)
$\lambda(t)$ is the removal rate of aerosols from the air (1/hr)
$S(t)$ is the source of aerosols into the containment as a function of time (g/m^3).

A temporal removal rate $\bar{\lambda}$ can be estimated using the MELCOR results at discrete times $(i, i+1)$.

$$\lambda_i \approx \frac{1}{\bar{C}_i} \cdot \left(\frac{S_{i+1} - S_i}{t_{i+1} - t_i} - \frac{C_{i+1} - C_i}{t_{i+1} - t_i}\right).$$

All values on the right hand side can be inferred from MELCOR output for a given scenario for all aerosol and vapor mass. The source mass, S, is inferred by performing a mass balance on the total aerosol/vapor mass present in containment (on heat structures, in pool, and airborne for all CNV control volumes).

Figure 5.4 and Figure 5.5 show the results of the staff's MELCOR calculations and the derived removal rate. The temporal removal rate $(\bar{\lambda})$ in Figure 5.4 is averaged over 30 minute intervals in Figure 5.5 to smooth the oscillations due to sensitivity to the discrete output time intervals and local containment thermal-hydraulic conditions.

In the above equations, the release to the environment from design-basis leakage was neglected. The design-basis leak rate (0.2 percent of containment volume per day or 1E-4/hr) is sufficiently small in comparison with the deposition rate (2/hr) that it can be neglected with no loss of accuracy in estimating the deposition rate.

One difference between the staff's MELCOR model and the applicant's STARNAUA model is that the staff's calculations do not include structural aerosol whereas the applicant's does. As a result, RAI 9224 requested the applicant provide the basis for inclusion of structural aerosol.

[redacted]

[redacted]

[redacted]

Figure 5.3 Containment removal rate and airborne aerosol concentration as reported in the Source Term Topical Report for NuScale.

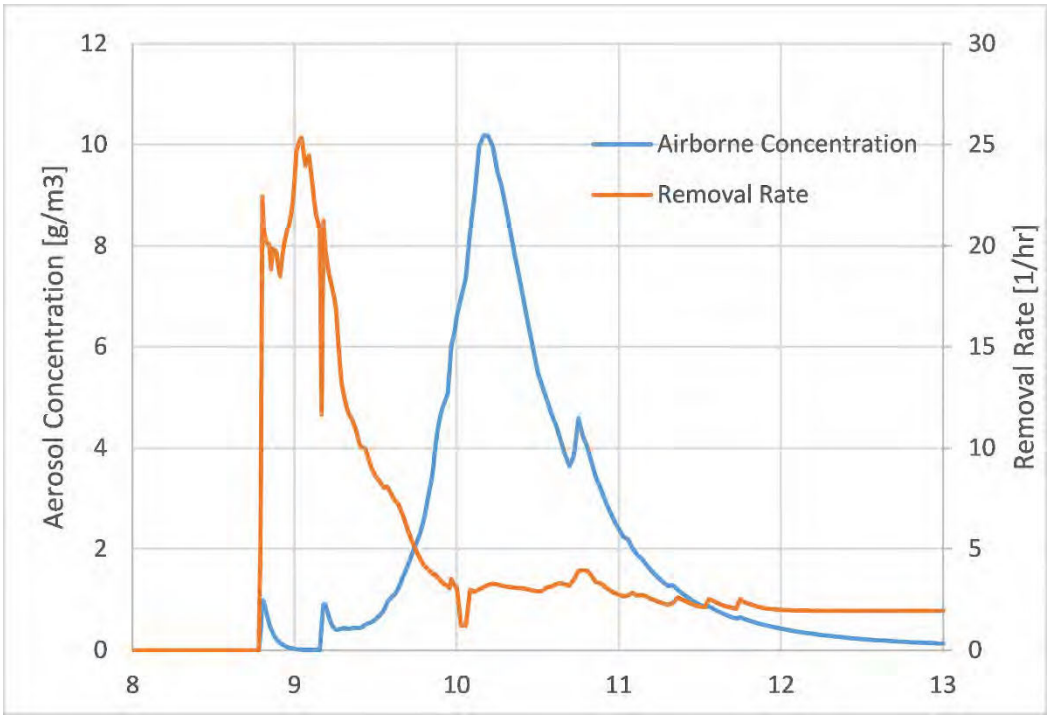

Figure 5.4 LEC-06T: Containment removal rate and airborne aerosol concentration.

[redacted]

[redacted]

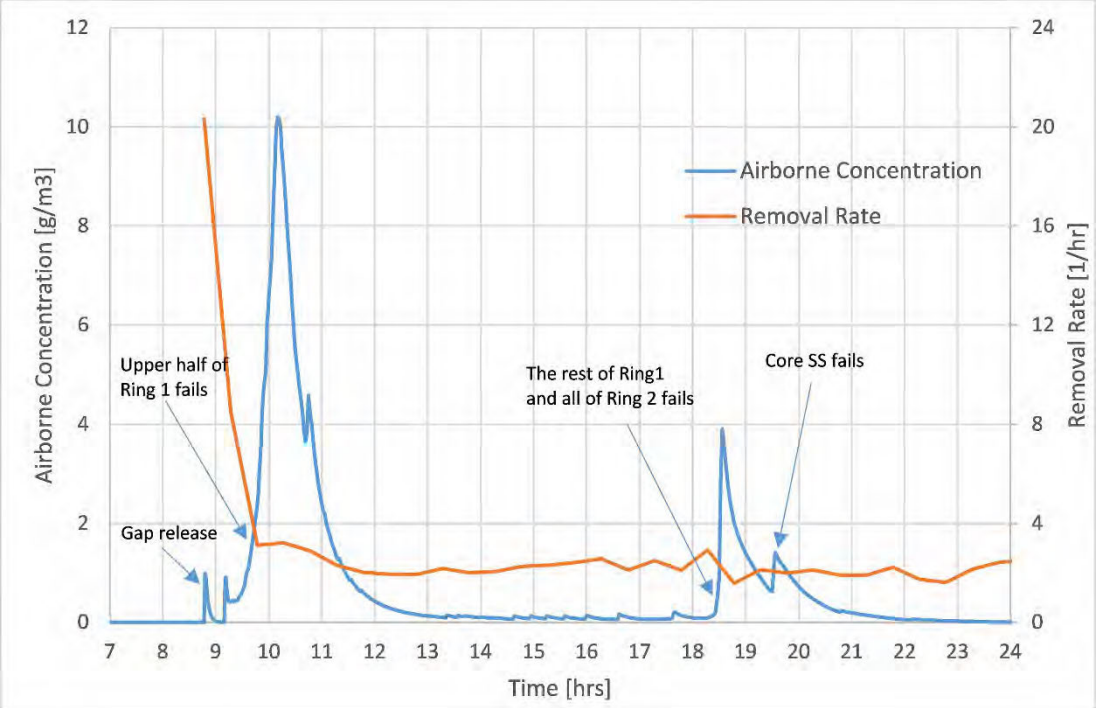

Figure 5.5 LEC-06T: Containment removal rate (averaged over 30 minute intervals) and airborne aerosol concentration.

5.4. Containment Leak Rate

The NuScale Accident Source Term Methodology topical report assumes that the containment leak rate is the design-basis leak rate of 0.2%/day and half that after 24 hours. In the staff's MELCOR model, the leak rate is directly modeled by a flow path from the upper containment atmosphere to the environment. The flow area of this path is chosen so that 0.2%/day leakage occurs when the containment is pressurized with air to the design pressure (1000 psia) and at a temperature of 70°F. These are the test conditions for the containment leak rate testing per Chapter 6 of the NuScale FSAR.

A comparison of the design basis leak rate and the staff's prediction for LEC-06T is given in Figure 5.6. The containment pressure and temperature for the staff's calculation is given in Figure 5.7. The leak rate calculated by the staff starts higher than the design basis leakage and then more than doubles in rate following core damage. The reason for this is multifaceted. The flow rate through the leakage path is dependent upon containment pressure, containment temperature, and material density which are all changing as the accident progresses. The elevated flow rate of 0.3%/day in the first few hours of the simulation is due to the high temperature of the containment atmosphere as compared to the test conditions. Figure 5.7 shows that the temperature is much greater than the test temperature of 70°F leading to a greater flow rate. As steam condenses, the CNV pressure falls and between 7.9 and 9.6 hours, the pressure in the CNV drops below the atmospheric pressure (Figure 5.7) and reverse flow through the leak path occurs (Figure 5.6). When core damage occurs and hydrogen is

[redacted]

[redacted]

generated through the zircaloy oxidation, the containment pressure and temperature increase. The containment leak rate increases rapidly as well. Even though the pressure and temperature after 10 hours is less than the initial value, the leak rate is more than twice as much. This is because of the much smaller density of the containment atmosphere at this time (see Figure 5.8) since it is composed mostly of hydrogen (molar concentration >0.8). See Appendix A for a demonstration calculation on the impact of vapor density on leak rate.

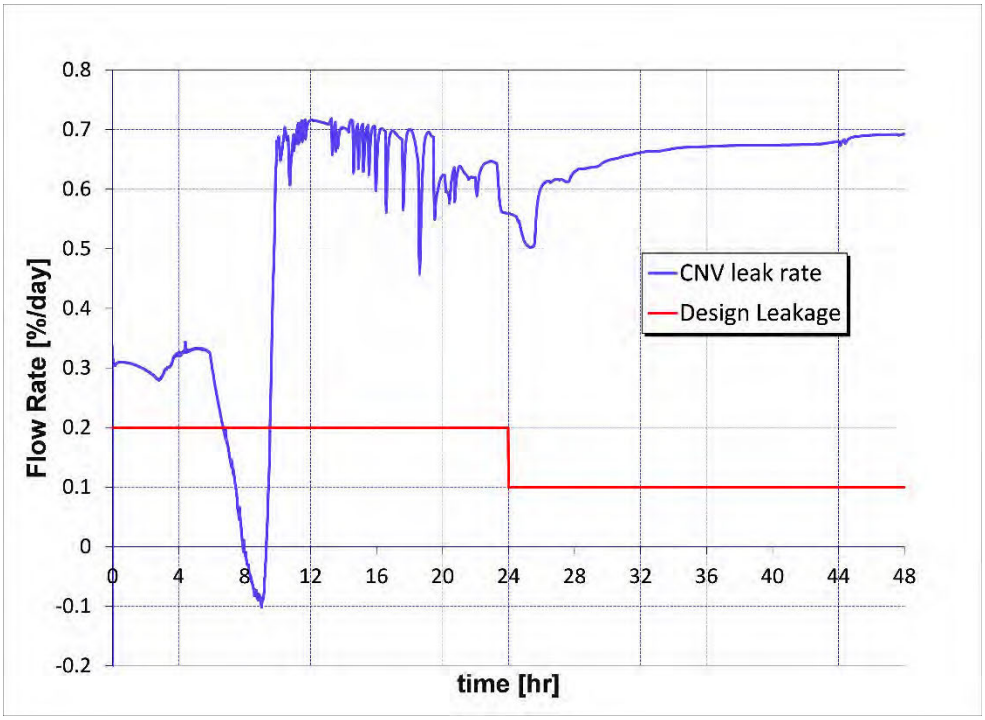

Figure 5.6 Containment leak rate calculated from staff's MELCOR calculation LEC-06T versus the applicant's assumed design leak rate.

[redacted]

[redacted]

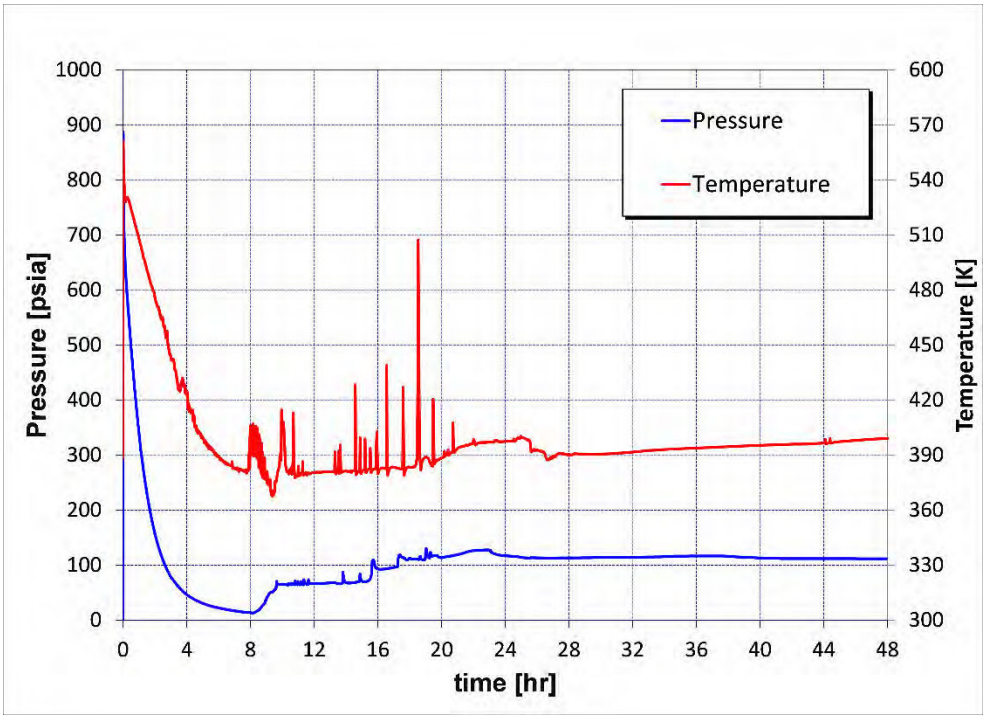

Figure 5.7 LEC-06T: Containment temperature and pressure.

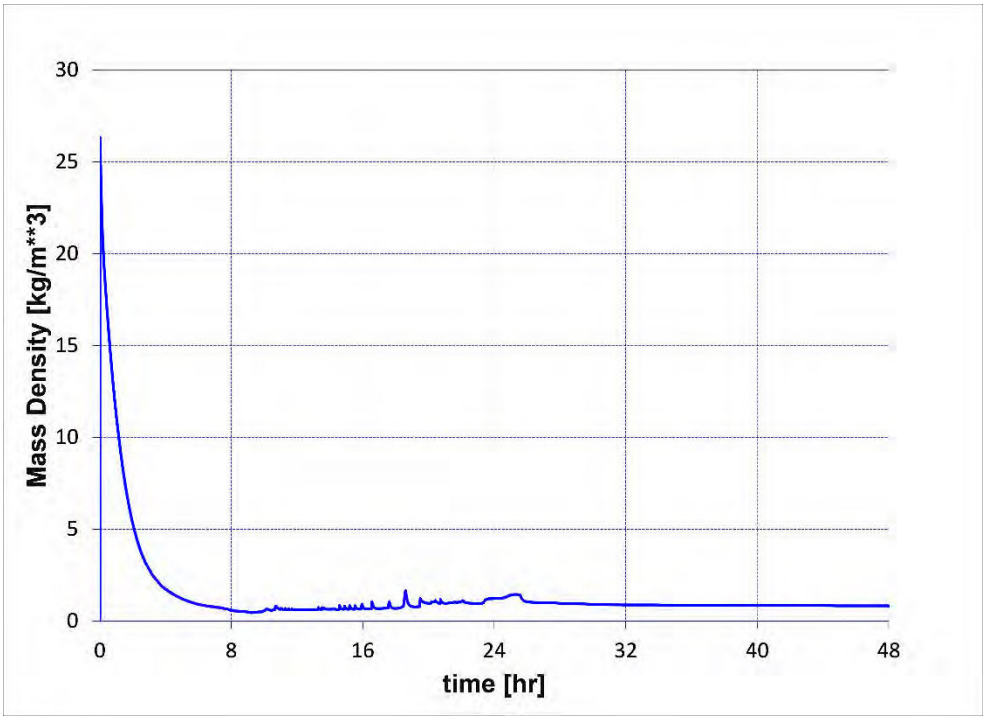

Figure 5.8 LEC-06T: Net mass density of materials in upper containment.

[redacted]

[redacted]

5.5. Release from the containment to the environment

Figure 5.9 presents the staff's results for the integrated fission product release from the containment into the reactor building for its MELCOR calculation for LEC-06T. Because the staff's MELCOR model assumes the containment leakage occurs at the top of the containment vessel, there is no scrubbing in the reactor pool. The results in Figure 5.9 can be used to confirm the applicant's analysis in its source term topical report (Reference 5) which is currently being updated and the applicant's analysis in its Environmental Report (Reference 4).

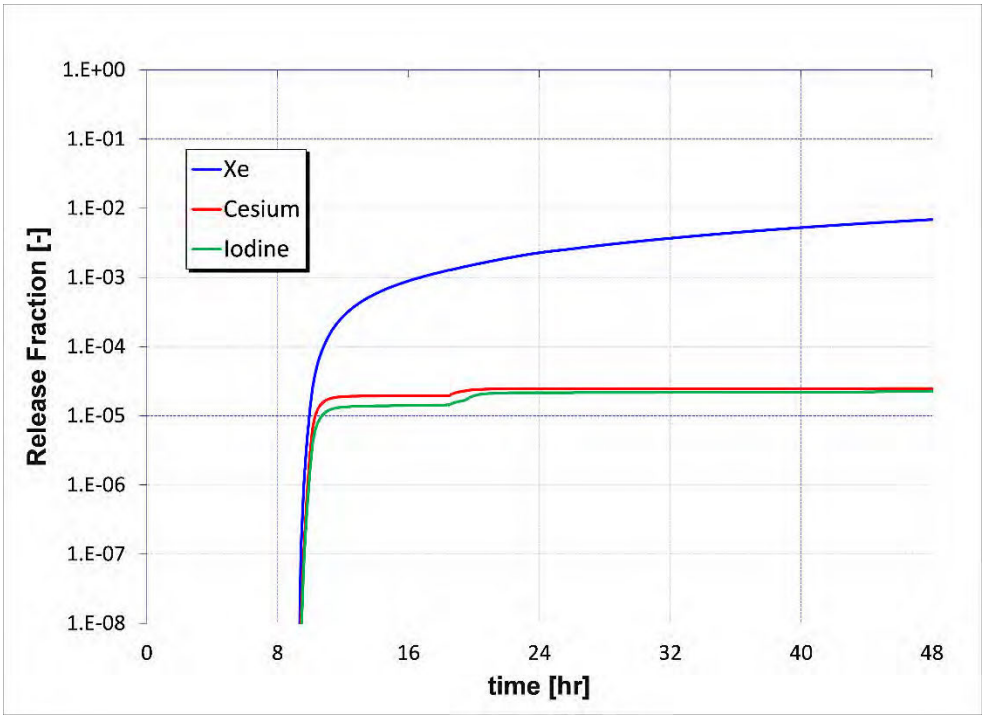

Figure 5.9 LEC-06T: Release fraction to the environment.

[redacted]

[redacted]

6. References

1. NuScale Final Safety Analysis Report, Revision 1, March 2018
2. “Calvert Cliffs, Units 1 & 2, Updated Final Safety Analysis Report”, Revision 48, September 14, 2015 (ADAMS No. ML15279A455)
3. “Updated MELCOR Calculation Notebook: NuScale Integral Pressurized Water Reactor,” ERI/NRC 13-205, Revision 7, December 2017.
4. “Applicant's Environmental Report - Standard Design Certification,” Rev 0, December 2016
5. Topical Report, TR-0915-17565, “Accident Source Term Methodology,” Revision 1, Non-Proprietary Version, April 8, 2016 (ADAMS Accession No. ML16099A394)
6. “Severe Accident Selection Methodology,” Rev 0, NuScale report ER-P020-4896-R0
7. “Dropped Module Consequence Analysis,” Rev 1, NuScale report ER-P060-7085-R1
8. “Probabilistic Risk Assessment Large Release Frequency Definition,” Rev 0, NuScale report ER-P000-7004-R0
9. “NuScale Power, LLC, Supplemental Information in Support of NRC Audit of Final Safety Analysis Report, Tier 2, Chapter 19 ‘Probabilistic Risk Assessment and Severe Accident Evaluation,’” letter from NuScale to NRC, August 3, 2017
10. “NuScale Power, LLC, Supplemental Information in Support of the NRC Audit of Final Safety Analysis Report, Section 19.2 ‘Severe Accident Evaluation,’” letter from NuScale to NRC, April 4, 2018
11. “U.S. Nuclear Regulatory Commission Audit of the Probabilistic Risk Assessment and Severe Accident Evaluation of the NuScale Power, LLC Design,” September 13, 2018 (ADAMS No. ML18254A340)
12. “Nuclear Regulatory Commission Audit of the Probabilistic Risk Assessment and Severe Accident Evaluation for the NuScale Design”, November 3, 2017, ADAMS No. ML17305A024
13. “Accident Radiological Analyses Sensitivity to Severe Accident Analysis,” Rev 0, NuScale report ER-0000-5278-R0

[redacted]

[redacted]

A. Example Problem of Containment Leak Rate

In order to demonstrate how the leak rate is affected by the conditions inside the containment, a simplied MELCOR model was constructed with two control volumes connecting to the environment. The flow paths have the same characteristics as the leak flow path in the NuScale input model. The control volumes are time independent with initial conditions shown in the figure below. CV400 represents the leak test conditions, while CV500 tries to mimic the conditions inside the NuScale containment following a severe accident. For simplicity, the material inside CV500 is assumed to be filled with hydrogen.

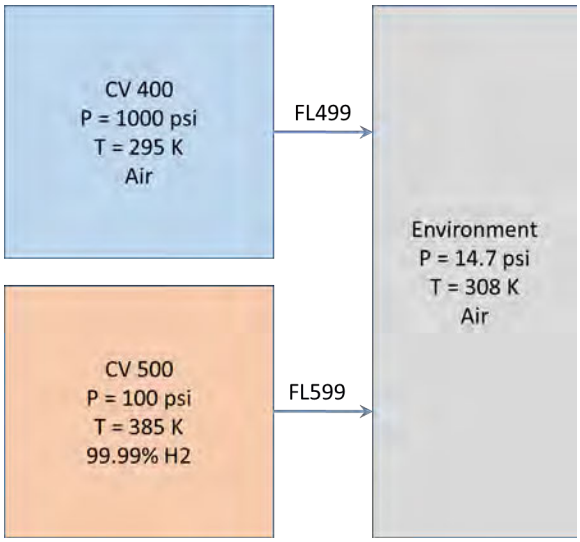

The code is run for 100 seconds and the results are show in the following figures. The resulting leakge rates are mostly consistent with the behavior in the NuScale analysis with FL499 calibrated to produce 0.2% leak rate and how the leak rate changes in response to changes inside the containment.

[redacted]

[redacted]

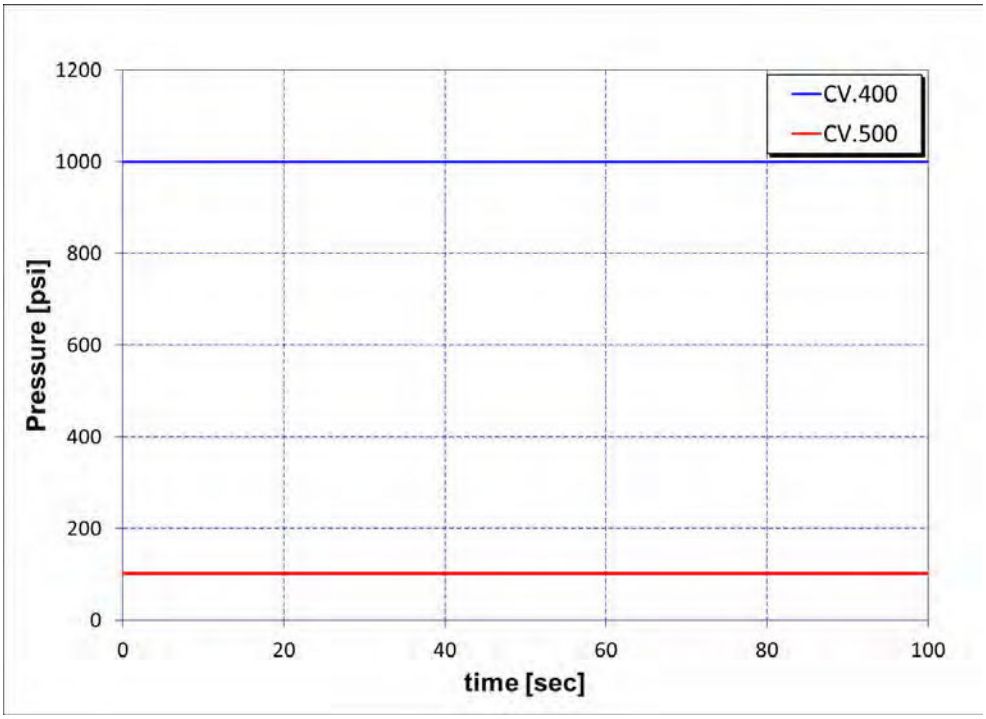

Figure A.1 Pressure history.

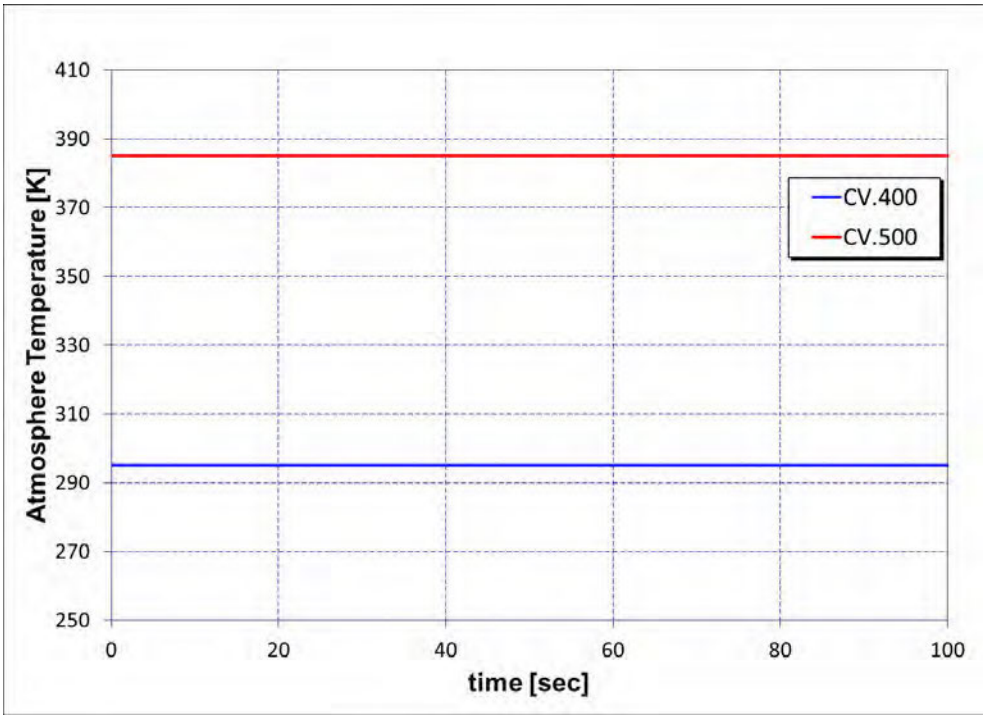

Figure A.2 Temperature history.

[redacted]

[redacted]

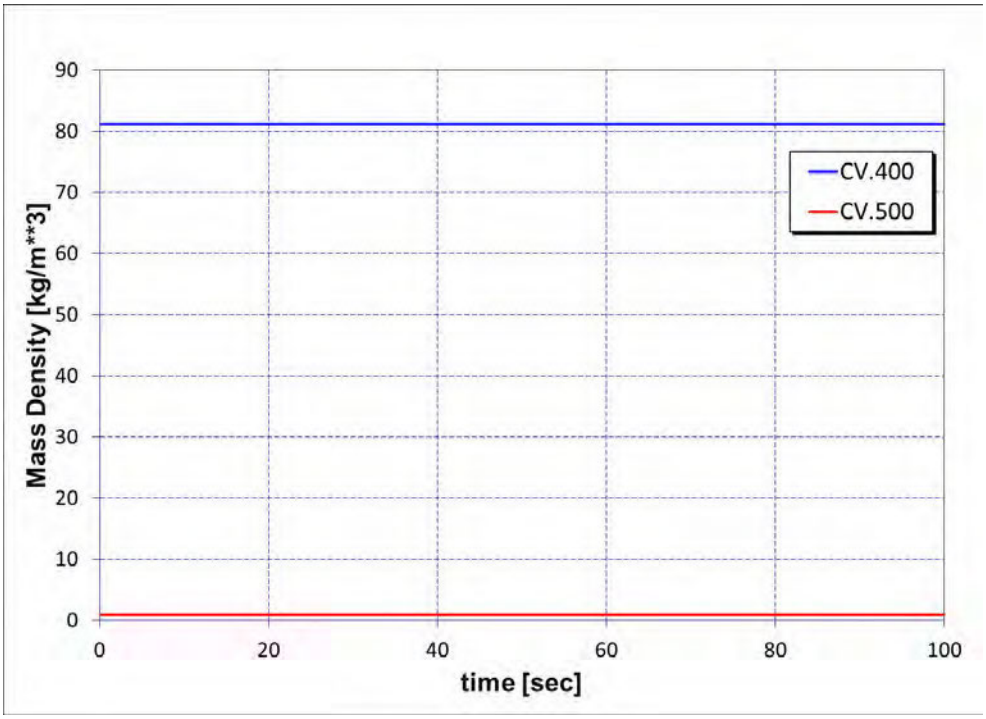

Figure A.3 Vapor density history.

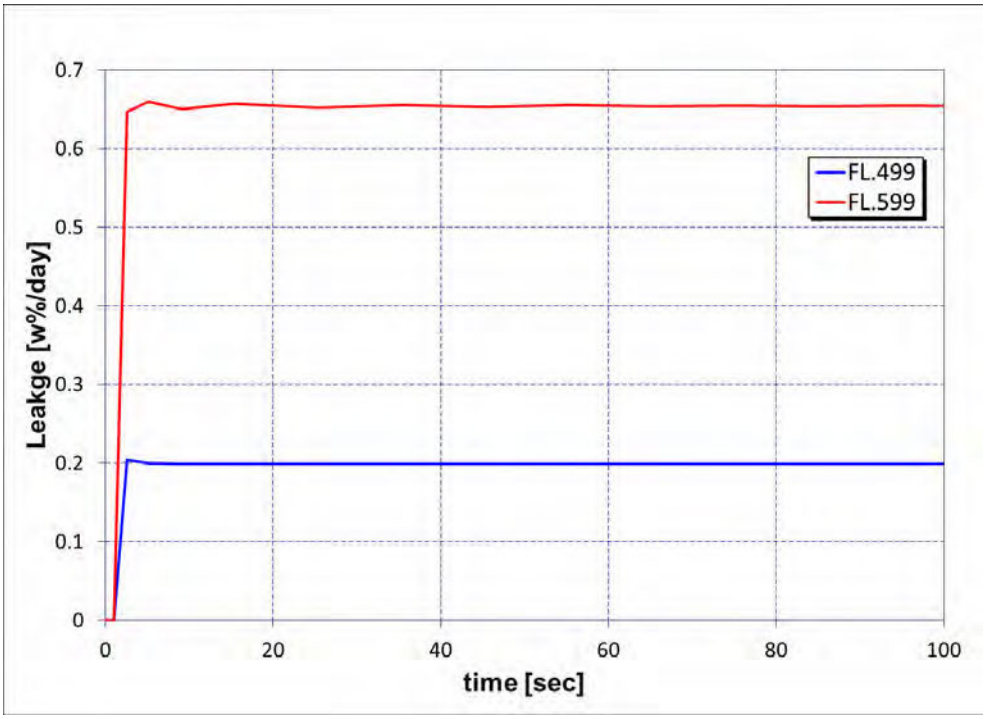

Figure A.4 Leakage flow rate history.

[redacted]